THE JOURNAL OF COMPARATIVE NEUROLOGY 508:153–174 (2008)

Sprouting Interneurons in Mushroom Bodies of Adult Cricket Brains

ASHRAF MASHALY, MARGRET WINKLER, INA FRAMBACH, HERIBERT GRAS, AND FRIEDRICH-WILHELM SCHÜRMANN
Johann-Friedrich-Blumenbach-Institut für Zoologie und Anthropologie, Universität Göttingen, D-37073 Göttingen, Germany

ABSTRACT

In crickets, neurogenesis persists throughout adulthood for certain local brain interneurons, the Kenyon cells in the mushroom bodies, which represent a prominent compartment for sensory integration, learning, and memory. Several classes of these neurons originate from a perikaryal layer, which includes a cluster of neuroblasts, surrounded by somata that provide the mushroom body's columnar neuropil. We describe the form, distribution, and cytology of Kenyon cell groups in the process of generation and growth in comparison to developed parts of the mushroom bodies in adult crickets of the species *Gryllus bimaculatus*. A subset of growing Kenyon cells with sprouting processes has been distinguished from adjacent Kenyon cells by its prominent f-actin labelling. Growth cone-like elements are detected in the perikaryal layer and in their associated sprouting fiber bundles. Sprouting fibers distant from the perikarya contain ribosomes and rough endoplasmic reticulum not found in the dendritic processes of the calyx. A core of sprouting Kenyon cell processes is devoid of synapses and is not invaded by extrinsic neuronal elements. Measurements of fiber cross-sections and counts of synapses and organelles suggest a continuous gradient of growth and maturation leading from the core of added new processes out to the periphery of mature Kenyon cell fiber groups. Our results are discussed in the context of Kenyon cell classification, growth dynamics, axonal fiber maturation, and function. J. Comp. Neurol. 508:153–174, 2008.

Indexing terms: adult neurogenesis; insect brain; Kenyon cells; f-actin

There is increasing evidence for de novo formation of neurons in mature brains of both vertebrates and invertebrates (Scharff, 2000; Cayre et al., 2002). Secondary neurogenesis is based on persisting neural stem cells that are part of the normal brain's cellular complement and that generate neurons throughout adult life (Cayre et al., 2002; Gould and Gross, 2002; Taupin and Gage, 2002). Furthermore, secondary neurogenesis in mature brains is generally not randomly distributed in diverse brain regions but is confined to some areas and neuron types (Cayre et al., 1996).

Mitotic activities and cell proliferation in adult insect brains were detected at an early stage (Panov, 1957) and studied comparatively (for review see Cayre et al., 2002). Neurogenesis in adult brains appears to be more widespread in hemimetabolous insects but is also encountered in forms with complete metamorphosis (Rossbach, 1962; Bieber and Fuldner, 1979; Cayre et al., 2002; Dufour and Gadenne, 2006).

In all cases studied, massive postlarval proliferation of neurons in adult insects has been identified in cell body clusters associated with the paired mushroom bodies (MBs). These neuropils are formed by a distinctive class of local interneurons, the Kenyon cells (KCs), and by relay neurons connecting the MBs with other brain regions. Different morphological classes of KCs (Schürmann, 1987; Strausfeld et al., 1998; Farris and Sinakevitch, 2003) emerge sequentially. They provide long axon-like processes, arranged in parallel that form these typical columnar neuropils. In the adult house cricket, KCs additionally

Dedicated to Franz Huber, Starnberg, Bavaria, a pioneer of insect neurobiology. Grant sponsor: Deutsche Forschungsgemeinschaft; Grant number: 723 Graduiertenkolleg (to F.-W.S.); Grant sponsor: State of Egypt (to A.M.).

*Correspondence to: Friedrich-Wilhelm Schürmann, Johann-Friedrich-Blumenbach-Institut für Zoologie und Anthropologie, Universität Göttingen, Berliner Straße 28, D-37073 Göttingen, Germany. E-mail: fschuer@gwdg.de

Received 29 June 2007; Revised 25 October 2007; Accepted 10 January 2008

DOI 10.1002/cne.21660

Published online in Wiley InterScience (www.interscience.wiley.com).

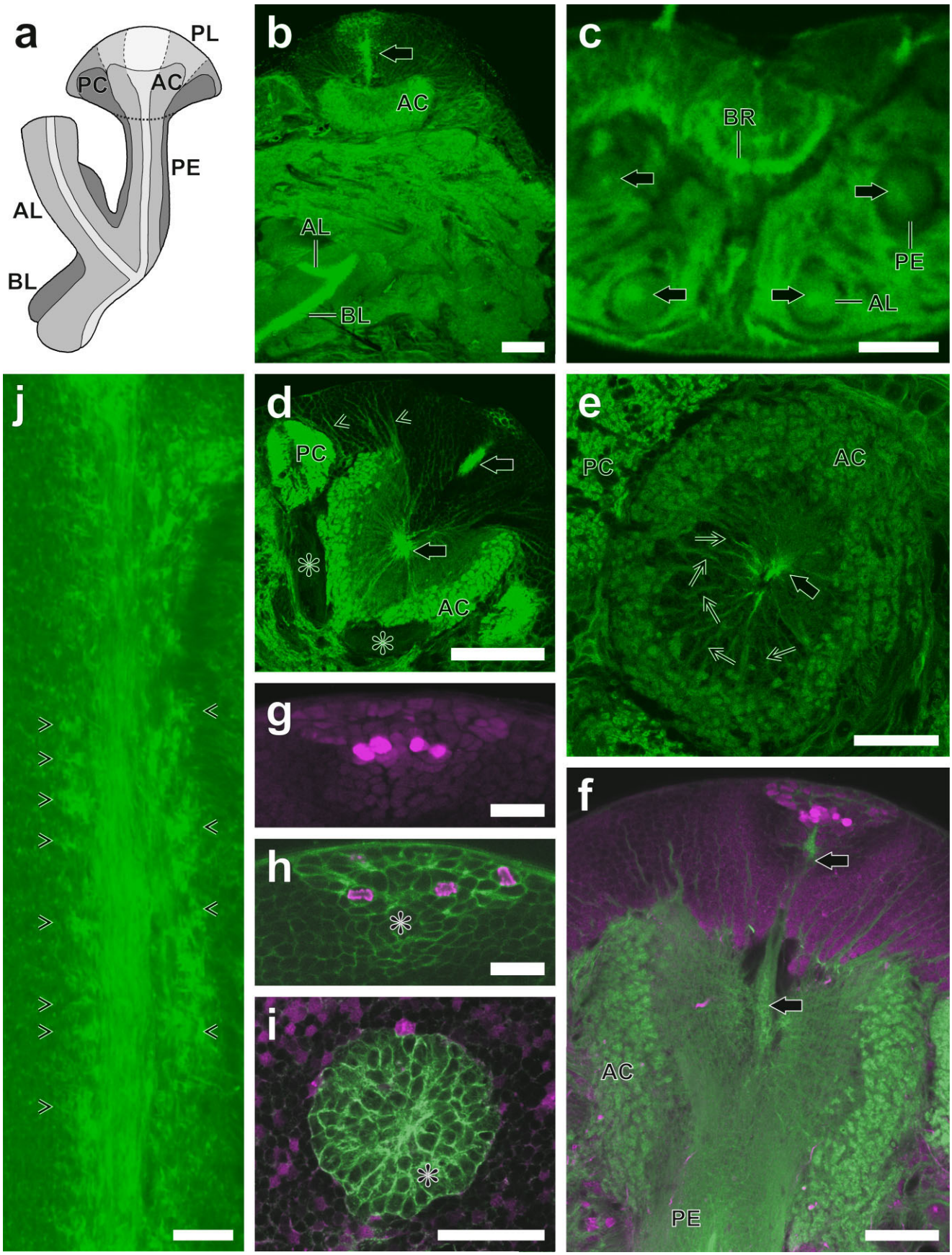

Figure 1

generated in the adult make up about 20% of an estimated total of 50,000 KCs in one MB (Malaterre et al., 2002). The neuroblasts and their progeny of the developing neurons are central in the mass of perikarya within the cup-shaped calyx. They give rise to a compact central core of fibers descending from the calyx into the stalk and lobes (see Fig. 1a).

MBs were earlier considered to be brain regions involved in the initiation and control of behaviors (Huber, 1960) or to represent major second-order neuropils involved in chemosensory and other sensory integration processes (Erber et al., 1987). Several studies have accumulated convincing evidence that MBs are centers required for some forms of learning and memory (Menzel, 2001; Pascual and Preat, 2001; Heisenberg, 2003; Schwärzel and Müller, 2006). Newly emerging neurons, growth processes, and even structural dynamics of synapses can be visualized by cellular and molecular marking techniques (Farris and Sinakevitch, 2003; Zhu et al., 2003; Martini and Davis, 2005). One molecule that indicates sites of neuronal growth and that is important for synaptic plasticity is f-actin (Matus, 1999; Dillon and Goda, 2005). This filamentous protein occurs at pre- and postsynaptic parts of neurons (Rössler et al., 2002; Dillon and Goda, 2005) and has been localized at KCs of certain species (Kurusu et al., 2002; Farris and Sinakevitch, 2003; Farris et al., 2004; Frambach et al., 2004). F-actin accumulates in dendritic tips of different KC types in some insect species but is dispersed within other MB regions (Frambach et al., 2004; Groh et al., 2004, 2006). The distribution and amounts of f-actin apparently depend on development and are specific for certain cell types within established functional networks of adult neurons.

The present paper describes structural characters of newly formed and sprouting KCs in the adult brain of an insect, the cricket *Gryllus bimaculatus*. For light microscopy, we used fluorescent phalloidin-f-actin staining and immunocytological approaches that indicate organelles and synapses. Synaptic sites in insect neuropil are often minute (Watson and Schürmann, 2002) and beyond the resolution limit of the light microscope. Therefore, to corroborate and verify light microscopic indications of synapses, organelles, and glia-neuron relationship, we also performed electron microscopic studies to resolve vesicles, organelles, and membrane specializations that together constitute typical synaptic sites. These ultrastructural investigations give further insight into KC growth and the integration of newly generated processes into established circuitry. Sampling by electron microscopy has provided measurable data for comparing KC fibers at different stages of development. A brief account of parts of this study has been published in abstract form (Mashaly et al., 2003).

MATERIALS AND METHODS

Animals

Male and female crickets of *Gryllus bimaculatus* were raised in the Institute's breeding colony at constant temperature (28°C) under a 12-hour/12-hour light/dark cycle. More than 110 adult animals (aged 1 week, 2 weeks, or 2 months after imaginal moult) and five last-instar larvae were used for light microscopy and 15 adult animals (aged 1 week, 2 weeks, or up to 2 months) for electron microscopy.

Histological and immunocytological procedures

Dissected brains from cold-anesthetized crickets were fixed overnight in 4% formaldehyde (freshly made from paraformaldehyde) in 0.1 M phosphate-buffered saline (pH 7.3 or pH 6.9 for histone immunocytology) at 4°C. Serial vibratome sections (30–50 μm) of the brains were subjected to phalloidin-f-actin staining and to immunocytological and other histological procedures. For f-actin detection, sections were incubated for 4 hours at room temperature with Alexa fluor 488-conjugated phalloidin (Molecular Probes, Eugene, OR; for details see Rössler et al., 2002). Propidium iodide (Sigma, St. Louis, MO; 20 μg /ml in PBS) without RNAse treatment was employed for staining nuclei and cytoplasm of neuronal and glial cells (for protocol see Devaud et al., 2003). For synapsin immunostaining, sections were permealized with 0.1% saponin

Fig. 1. **a:** Scheme of one of the paired mushroom bodies with Kenyon cell perikaryal layer (PL) and neuropil compartments of the anterior calyx (AC) and posterior calyx (PC), pedunculus (PE), α-lobe (AL), and β-lobe (BL). Note that the distinct Kenyon cell fiber bundle (dark areas) descending from PC along lateral parts of PE does not ascend to the top of AL and occupies a medial position in BL (γ-lobe division); fibers of developed (gray areas) and of growing Kenyon cells (white areas) descending from AC end at the top of AL and BL. These abbreviations are also used in the subsequent figures. b–j: Differential f-actin distribution in the mushroom bodies and surrounding neuropil. Phalloidin-f-actin staining (green) of vibratome sections (thickness 30–50 μm); confocal images. **b:** Intense labelling of a compact fiber bundle (arrow) emerging from a central peripheral cluster of sprouting Kenyon cells projecting through AL and BL. Frontodiagonal section. **c:** The intensely labelled fiber bundle (central core area, arrows) is found in PE and AL. Strong staining of the bridge (BR) of the central complex neuropil. Horizontal section. **d:** Mushroom body calyx at higher magnification. Strong labelling of central core elements (arrows) in the perikaryal layer (PL) and in the peripheral glomerular layers of AC and PC. Massive Kenyon cell fiber bundles (asterisks) descending from PC to upper PE appear mainly free of f-actin. Note stained fiber bundles of developed Kenyon cells (arrowheads) in peripheral parts of the somatic layer. Frontal section. **e:** Cup-shaped anterior calyx showing tiny fascicles (thin arrows) projecting from the center (thick arrow) to the glomerular layer of AC (compare e,f). Horizontal section. f–h: Additional Kenyon cell labelling with antiphosphohistone mitosis marker (magenta). Strong staining of large mitotic somata in the cluster of sprouting Kenyon cells together with weakly stained small Kenyon cell somata. **f:** The growing cells in the somatic layer of Kenyon cells form a massive central bundle of f-actin-stained fibers (arrows) descending through the inner nonglomerular part of AC to the central part of the PE cylinder. F-actin-stained centrifugal fascicles running to the glomerular AC were detected in the calyx exclusively, never in PE, AL, or BL. Frontal section. **g,h:** Mitotic nuclei in the cluster of developing cells (asterisk); in g gamma value 1.6. Frontal section. **i:** Net-like f-actin staining in the conic cluster of presumptive Kenyon cell somata (asterisk). Some Kenyon cell somata (magenta) were labelled with fluorescent dextran by axonal back-filling at the top of AL. They were found not within the f-actin web but outside its rim. Horizontal section. **j:** Portion of the central core area of PE with lateral protrusions (arrowheads). Longitudinal section at high magnification. Scale bars = 50 μm in b–f,i; 20 μm in g,h; 5 μm in j.

(Sigma) and, for blocking, were treated with 1% bovine serum albumin (BSA) buffer for 1 hour and subsequently incubated with a monoclonal antibody directed against *Drosophila* synapsin I isoform (SYNORF1; dilution 1:1,000 in 0.5% blocking buffer, at 4°C overnight; for a detailed protocol see Fabian-Fine et al., 1999). The antiserum SYNORF1 (kindly provided by Dr. Buchner, Würzburg, Germany) was raised by Klagges et al. (1996) against a fusion protein consisting of glutathione-S-transferase and synapsin protein. The antibody specificity was confirmed in *Drosophila* nervous tissue by the absence of immunolabelling in mutants lacking synapsin (Godenschwege et al., 2004). The antibody directed against *Drosophila* synapsin, marking brain compartments in *Drosophila* (Godenschwege et al., 2004), has been used for selectively labelling neuropil with synaptic vesicle pools in several arthropods (crustaceans: Harzsch et al., 1997; spiders: Fabian-Fine et al., 1999; insects: Frambach et al., 2004; Leitinger et al., 2004), including also corresponding MB compartments in bees and crickets (Frambach et al., 2004; Okada et al., 2007). Synapsin-like labelling was visualized using goat-anti-mouse IgG coupled to Cy3 (dilution 1:100; Jackson, Dianova; Hamburg, Germany). By light microscopy, immunostaining of the cricket MBs gave results identical to those of our previous study (Frambach et al., 2004). Selective marking of synaptic vesicle-containing fiber profiles by immunoelectron microscopy has previously been demonstrated in MBs of the cricket (Frambach et al., 2004) and for grasshoppers (Leitinger et al., 2004), whereas fibers devoid of vesicles were not stained.

α-Tubulin was demonstrated immunocytochemically using a monoclonal antibody directed against acetylated α-tubulin (dilution 1:1,000; product No. T6793; Sigma). Acetylated tubulin from the sea urchin *Strongylocentrotus purpuratus* was used as the immunogen, and a monoclonal antibody against acetylated tubulin (mouse IgG2b isotype) was derived from the hybridoma produced by fusion of mouse myeloma cells from immunonized mouse. The antibody has been successfully employed to detect acetylated α-tubulins from various organisms, including protista, plants, invertebrates, and vertebrates (Le Dizet and Piperno, 1987). It stains selectively tubulins in arthropods (Harzsch et al., 1997; Tucker et al., 2004) and annelids (Voronenzhskaya et al., 2002), especially in nerve cell somata and in axonal fibers with gathered microtubuli. Therefore, tracts and nerves can be visualized and traced similarly to tracing in silver- or gold-stained insect nervous systems (see Strausfeld, 1976). Tubulin labelling was performed according to the protocol used for nerve cells and neuronal tracts (Harzsch et al., 1997). For tubulin/phalloidin-f-actin double labelling, Alexa Fluor 488-conjugated phalloidin was added to the secondary antibody as described for synapsin labelling. Omission of the first antitubulin antibody prevented staining of tracts.

Mitotic cells in the MBs were detected by immunocytochemistry with a rabbit polyclonal antiserum against phosphorylated histone H3 (lot 23 136, Upstate Biotechnology, Lake Placid, NY). This antibody recognizes specifically histone H3 of approximately 17 kD (immunogen KLH-conjugated peptide, corresponding to amino acids 7–20 of human histone H3) during mitosis and has been shown to mark mitotic chromosome condensation in a wide range of eukaryotes, including insects (Hendzel et al., 1997). It labels dividing MB KC neuroblasts in pupal stages (Malun et al., 2003). Mitotic events visualized by immunocytochemical histone marking (this study), exclusively in the KC proliferation zone of adult cricket mushroom bodies, have been correspondingly shown at the same site with the 5-bromo-2′-deoxyuridine (BrdU) technique (Cayre et al., 1996). Thoroughly rinsed vibratome slices were preincubated in 5% normal goat serum (NGS) in PBS containing 0.1% Triton X-100 for 1.5 hours before incubation with antiphosphohistone H3 mitosis marker (dilution 1:200 in PBS) for 24 hours (for details see Harzsch et al., 1999; Malun et al., 2003). For visualization, Cy3-conjugated goat anti-rabbit secondary antibody was used. To label KC fibers and somata, small pieces of crystalline dextran conjugated with tetramethylrhodamine (3,000 MW; Molecular Probes) were placed on top of the α-lobe within excised brains kept in insect Ringer saline. After incubation for 1.5–3 hours, brains were fixed with paraformaldehyde and sectioned as described above.

Double-labelling experiments (phalloidin/synapsin, phalloidin/tubulin, phalloidin/histone) were performed by adding phalloidin solution to the secondary antibody solution for 5 hours or as a second subsequent procedure (dextran/phalloidin). Sections were mounted in buffer-glycerol solution (1:3).

Light microscopy and image improvement

Conventional brightfield and fluorescence microscopy was performed on a Zeiss Axioskop with a HBO50 mercury lamp and Plan-Neofluar optics. Images (eight bits per colour channel, 1,315 × 1,033 pixels) were taken with a cooled Spot CCD camera (Diagnostic Instruments). Generally, we improved intensity and contrast by linear operations (additive and/or multiplicative) on the whole image area to make optimal use of the eight-bit range of pixel values. Median 3 × 3 filtering was applied to some images. Any other nonlinear modification (gamma adjustment) is specified in the legends of the figures to which it applies.

Excitation wavelengths of 488 nm and 543 nm were used on a Zeiss LSM510 laser scanning confocal microscope equipped with 10/0.3 (dry) and 40/1.3 (oil) Neofluar objectives. Usually, images (eight or 12 bits/pixel, 512 × 512 or 1,024 × 1,024 pixels) were recorded with the pinhole closed to 1 Airy unit and in sequential scanning mode for double-stained preparations. Occasionally, 3 × 3 median filtering was applied for noise reduction. Most images were enhanced by a linear stretch of the look-up table (LUT) so that approximately 0.1% of all pixels were brought to saturation (Photopaint 8; Corel). However, with stacks of consecutive optical sections, application of the same LUT to all sections often results in dark images of low contrast from within the vibratome slice. When the general histological structure of the preparation is fairly homogeneous throughout the recorded stack, the intensity histogram is expected to be the same at each z-level, and any deformation of the intensity distribution will be caused by unavoidable variations in illumination, fluorophore concentration, and light detection, depending on tissue thickness. To compensate for these complex and interacting effects, the individual LUT of each image was nonlinearly transformed to adjust the cumulative histogram of pixel intensities to that of a reference image, usually the brightest image of the focus series. This computationally fast method (H. Gras, unpublished), which avoids operator bias during image correction, was imple-

mented in the script language of ImageTool2.0 (http://ddsdx.uthscsa.edu/dig/itdesc.html).

Electron microscopy, image improvement, and quantitative analysis

Brains were immersed in a fixative of 2.5% glutaraldehyde in 0.1 M phospate buffer (pH 7.4) overnight and postfixed in 2% OsO_4 for 2 hours following standard protocols (Robinson et al., 1987). Araldite-embedded total brains were cut using a diamond knife (frontal, sagittal, and horizontal section planes). For inspection of MBs, samples from 15 brains were examined. Horizontal serial semithin sections of the MB were achieved for one animal aged 1 week. Ultrathin sections (diameter 50–60 nm) were taken at intervals of 20 μm and mounted on slot grids in order to obtain total cross-sections of MB neuropil and contrasted with uranyl acetate and lead citrate. Sections were inspected and photographed using plates (size 8 × 10 cm) at primary magnifications ranging from ×2,500 to ×20,000 with a Zeiss EM 10B or Zeiss CEM 902A. To study changes in cross-sectional area of KCs and number of microtubules per fiber in the stalk, a linear sequence of micrographs (primary magnification ×10,000) was taken from the center to the periphery from one section. Images of similar size were selected every 3.5 μm and digitized at 1,200 dpi from the negative (Epson Perfection 2450 scanner), improved and analyzed with Photopaint 11 (Corel), Photoshop 7 (Adobe), and dedicated scripts for ImageTool2.0, followed by numerical data transfer to Excel (Microsoft) and Origin (Microcal) for further computations and display. In detail, we performed the following operations: After optional flat-field correction to compensate for intensity loss at the periphery of the image, the contrast was increased by adjusting the intensity of each pixel between 0 and 255 proportional to the minimum and maximum intensities found in its n × n neighborhood (n = 31, 51, or 71). The resulting image was binarized to detect the dark membranes, followed by a "close" operation to fuse disconnected elements. Combined as semitransparent red overlay with the contrast-enhanced original, the image was controlled for residual mistakes and manually corrected with white or red lines, respectively. The red channel of the verified RGB image was again binarized so that subsequent object detection identified areas of cytoplasm (fiber cross-sections), rejecting objects in contact with the image border. Automatic object analysis (ImageTool 2.0) finally determined some numerical parameters, of which only fiber number and fiber area are used in this study (see Fig. 12). Structural complexity and uneven electron density in different micrographs prevented a reliable automatic detection of microtubules, so they were counted manually within the same fibers. Similarly, from other micrographs (primary magnification ×4,000) numbers of synapses and mitochondria in different regions of one MB were counted manually within consecutive 3 × 3 μm^2 squares placed along a line between central fiber bundle and periphery (see Fig. 13).

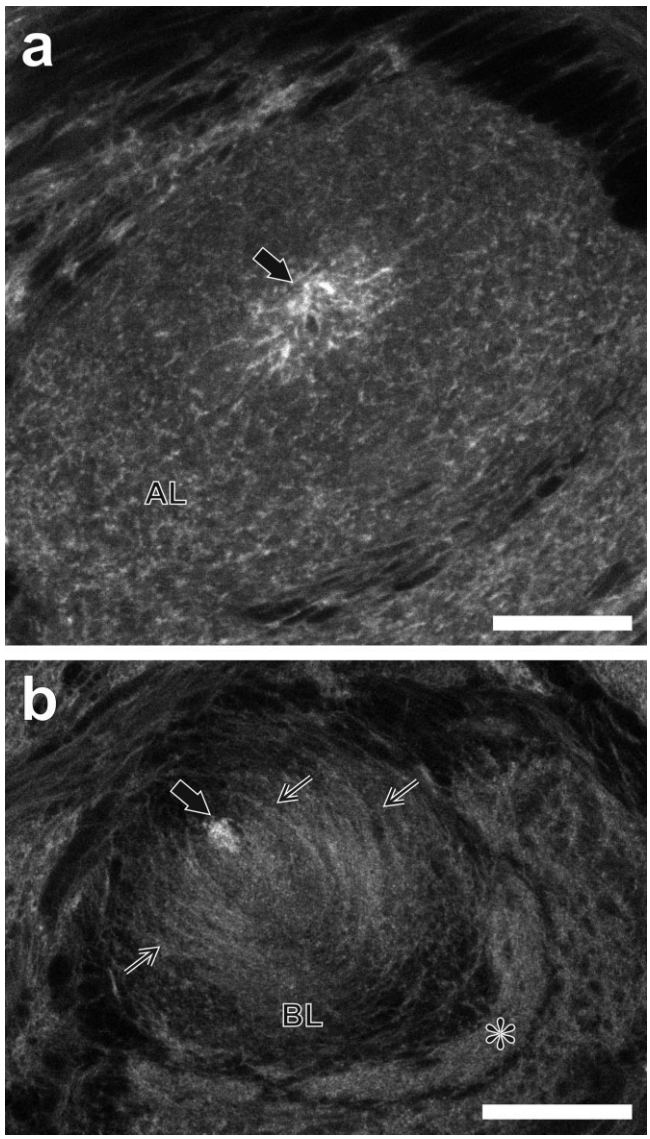

Fig. 2. Phalloidin-f-actin labelling in cross-sections of AL and BL. **a:** Upper part of AL; intensely labelled centrifugal projections from the central core (arrow). Note f-actin stained elements throughout the AL neuropil. **b:** Lateral position of central core area (thick arrow) in BL. Note strong staining of longitudinal fibers (thin arrows). Compact f-actin labelling in medial parts of BL (asterisk). Scale bars = 20 μm in a; 50 μm in b.

RESULTS

F-actin in the MBs

Fluorescent phalloidin-f-actin staining marks neuropil compartments (Rössler et al., 2002) and even distinct differences of f-actin distribution at the nerve cell level (Frambach et al., 2004). Longitudinal subdivisions of the cricket's MBs are also discriminated by phalloidin-f-actin labelling (Figs. 1, 2). In cricket MBs, separate anterior and posterior perikaryal areas (Fig. 1a) give rise to three classes each with separate distributions in the MB's subdivisions (Schürmann, 1973; Schürmann et al., 2000; Frambach et al., 2004). Large class III KC neurons extend their spiny dendrites into the posterior calyx, and their bundles of descending axons form the marginal peduncu-lus and peripheral parts of the α-lobe (vertical lobe) and β-lobe (medial lobe). Class II and class I KC dendrites are restricted to the anterior calyx. Their descending axons

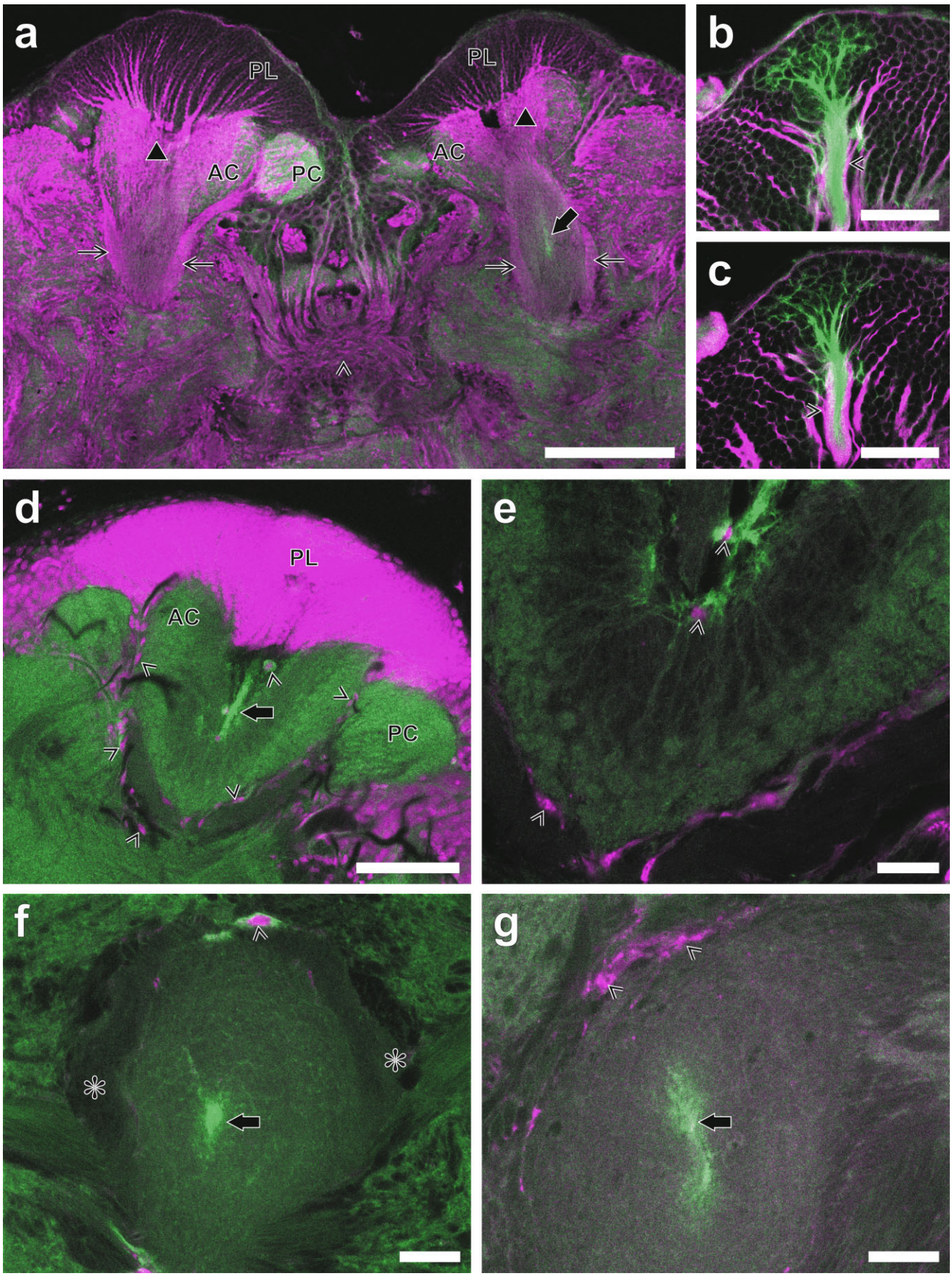

Figure 3

form the major part of the pedunculus and a columnar subdivision in the α-lobe and β-lobe. Tiny fibers of class I KCs form bundles at the central (core) parts of the pedunculus, α-lobe, and marginal ventrolateral portions of the β-lobe.

In last-instar larvae and throughout adult life, proliferating KCs, which are revealed by BrdU labelling (Cayre et al., 2002) and by antibodies against phosphohistone mitosis marker, are confined to a cone-like cluster that is centrally located among KC perikarya within the cup-shaped anterior rind (Fig. 1b,d,g–i). No mitotic events have been found within class III KCs in mature brains. F-actin staining of proliferating cells appears as a net-like area (Fig. 1h,i), prominent against the surrounding older and more developed neurons. Perikarya of this proliferation zone could not be stained with fluorescent dextran by back-filling experiments via the α-lobe top (Fig. 1i). In contrast, dextran-labelled KC somata at the margin of the f-actin web-like arrangement reveal axon-like processes fully extended into the stalk and lobes. The cluster of perikarya of developing KCs, which shows strong phalloidin-actin staining, gives rise to a compact bundle of KC processes, which can be followed through the central anterior calyx, into its stalk, and then to the tips of the lobes (Figs. 1b,c,f, 2). This intensely stained central core of processes is of a cylinder-like form (diameter 5–8 μm) with fuzzy margins (Figs. 1j, 2) and is equipped with radial extensions in the anterior calyx and lobes. This bundle is surrounded by unlabelled axon-like processes of developed KCs.

In the anterior calyx, small phalloidin-actin-stained fascicles (diameters up to 2 μm) emerge from the central core fiber bundle (Fig. 1d–f) and project radially toward the microglomeruli in the anterior calyx, each microglomerulus representing the site of convergence between a bouton from an antennal lobe projection neuron and the postsynaptic spines of KC dendrites (Schürmann, 1974; Yasuyama et al., 2002). The fuzzy margin of the central core fiber bundle suggests sprouting of collaterals from the thin axon-like processes of developing KCs into the surrounding ensembles of mature KC axons. The microglomerular organization of the anterior and posterior calyx is revealed by their strong phalloidin-actin affinity (Fig. 1b,d–f), which accumulates at subsynaptic tips of the KC dendrites (Frambach et al., 2004). Other elements that stain with phalloidin-f-actin, but not as intensely as those stained within the central core, occur around the margins of the core (Figs. 1f, 2) in locations where synapses are first encountered (see below).

Antitubulin immunocytochemistry (Fig. 3a–c) reveals bundles of KC fibers that are arranged in parallel and suggest an affinity with mature KCs. For example, the cluster of newly emerging KC perikarya appears to be mainly free of tubulin-like immunostaining. Antitubulin labelling analyzed in stacks of confocal images could only partially be related to core fiber bundles rich in f-actin, and these were mainly at the margin of the core. Beyond the margin, KCs show strong affinity to antitubulin.

We found variable labelling of the perilemma sheath by phalloidin-actin and by antitubulin antibody reactivity (Fig. 3a–c). Glial and tracheal cell nuclei were clearly labelled by propidium iodide staining (Fig. 3d–g). These elements are located at the border between the cell body (perikaryal) rind and neuropil. They also demarcate discrete neuropils as well as subdivisions within the MB itself. Confocal imaging was unable to detect actin-rich glial protrusions that invade MB neuropil, although minute glial extensions are seen in electron micrographs. We suggest that the radial phalloidin-f-actin-positive fascicles in the anterior calyx are neuronal elements. We have so far considered prominent amounts of f-actin in MB in calycal microglomeruli, at KC dendrites, and in the central core area, composed of gathered fibers of sprouting KCs, besides other neuropil areas of weaker phalloidin-f-actin staining in MB subdivisions containing synapses of intrinsic and extrinsic neurons.

Synapsin distribution

Occurrence and distribution of putative synaptic sites were investigated immunocytochemically by light microscopy employing an antibody raised against *Drosophila* synapsin (Klagges et al., 1996), which in crickets specifically marks presynaptic sites filled with synaptic vesicles and presynaptic boutons in MBs of bees and ants (Frambach et al., 2004). Synapsin-like immunolabelling is absent in the core of developing and sprouting KC processes (Fig. 4a,b). High-resolution confocal images collected from stacks revealed small synapsin-like spots in the anterior calyces adjacent to phalloidin-f-actin-stained fascicles. These fiber bundles project radially from the central core to the peripheral zone of synaptic microglomeruli (Fig. 4c–g). Because of the limitations of resolution, it was not possible to determine whether the synapsin-immunoreactive spots were situated within phalloidin-f-actin-stained dendritic elements. These putative synaptic complexes also appear to occur separately from phalloidin-f-actin-stained fascicles (Fig. 4g). Minute presynaptic spots were also detected within subdivisions of the lobes equipped with axon-like processes from class II KCs (Fig. 4h). In the α- and β-lobes (Fig. 4i,j), which are packed with axon-like KC processes that contain abundant presynaptic vesicles (Schürmann, 1972, 1974), synapsin-like spots could not be analyzed in

Fig. 3. a–c: Phalloidin-f-actin (green) and tubulin (magenta) double labelling of mushroom bodies and neighboring neuropil. **a:** In the perikaryal layer (PL), Kenyon cell axons are gathered into fiber bundles descending to the inner parts of AC (triangles), and compact bundles project from the PC (thin arrows) to lateral parts of the PE. In the central core (thick arrow) f-actin labelling is preponderant; fiber tracts free of antisynapsin labelling appear magenta. Synaptic neuropil of the glomerular calyx parts (AC; PC) and other areas of the brain always contains considerable amounts of f-actin. Note chiasmatic fibers of the central complex (arrowhead). **b,c:** The conic cluster of sprouting cells and its emerging compact central core complex show strong phalloidin f-actin labelling. The central core is here accompanied by circumferential fiber bundles (arrowheads) of more developed, older Kenyon cells. Frontal sections; images from different stack levels; b: maximum projection of four sequential slices through an optical depth of 4 μm; c: single slice of 1 μm optical depth. d–g: Labelling of f-actin (green) and of somata with propidium iodide (magenta). **d:** The PL of Kenyon cells and glial cells in the neuropil at borders of compartments (arrowheads); central core (arrow). **e:** Glial somata (arrowheads) at the central core and at margins of AC; same vibratome slice as in d. **f:** Glial cell (arrowhead) at the PE border with high f-actin labelling; lateral fiber bundles of large Kenyon cells (asterisks) from PC devoid of synapses show only weak f-actin staining, whereas the inner parts of the PE with Kenyon cell fibers from AC are clearly labelled; strong f-actin staining of the central core (thick arrow). **g:** Upper α-lobe (cross section) with glial cells at its border; center marked by arrow. Scale bars = 100 μm in a,d; 50 μm in b,c; 20 μm in e–g.

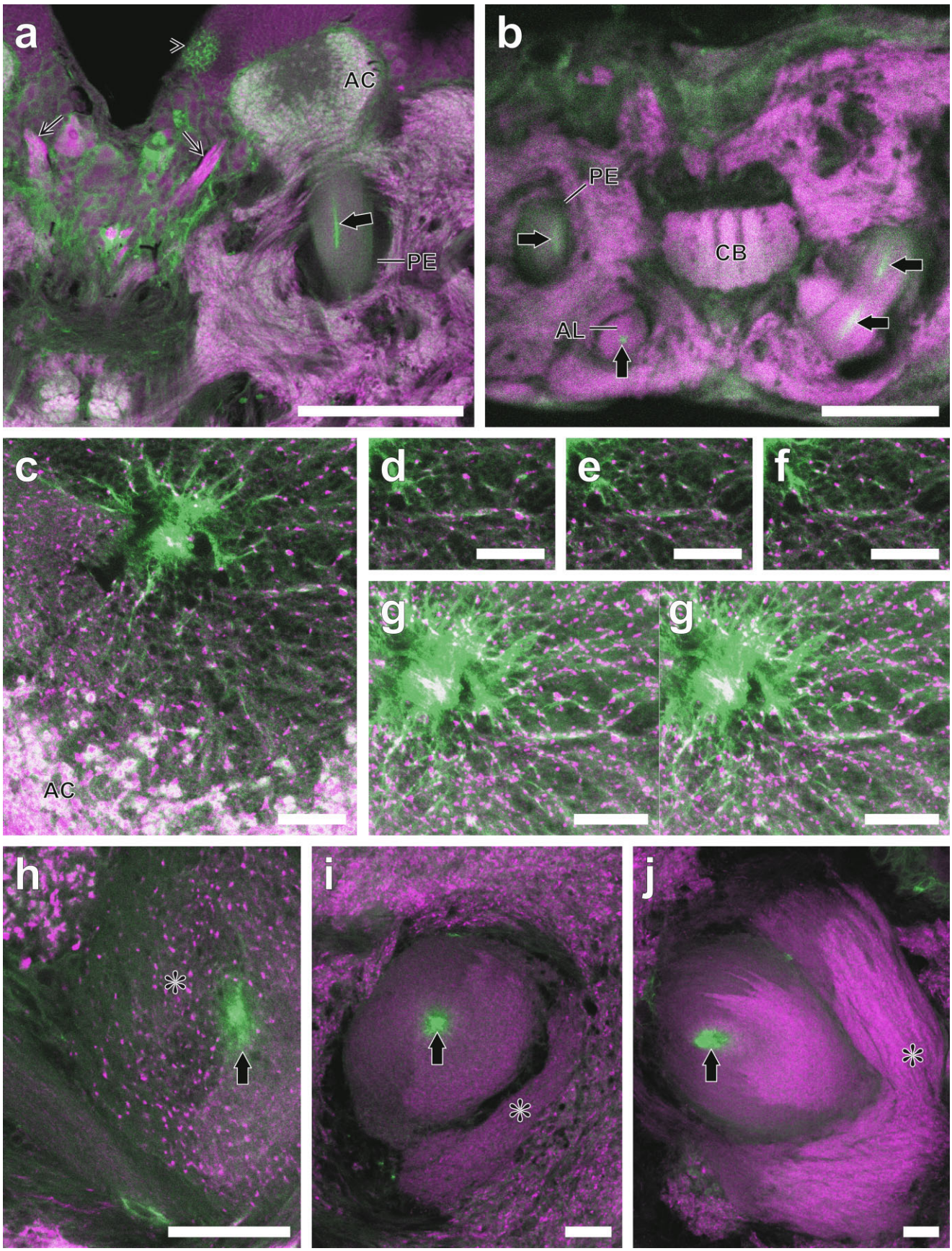

Figure 4

sufficient detail by confocal imaging. However, it is obvious that synapsin is nonhomogeneously distributed in the subdivisions of the lobes (Fig. 4i,j). Synapsin-like staining patterns change along the length of the vertical and medial lobes. The core bundle of sprouting and developing KC processes is devoid of synapsin label. Also, extrinsic fibers invading the central core of the calyces, pedunculi, and lobes were not detected by light microscopy.

Ultrastructure of growing and mature KCs

Sprouting KC axonal fibers can be discriminated from older KCs not only by light but also by electron microscopy because of their prominent density (Figs. 5–10). Systematic investigation of sprouting KCs in the core fiber bundle compared with other KCs outside the core was facilitated by the neat concentric organization of KC processes. Special attention was given to the expression of ribosomes, rough endoplasmic reticulum, microtubules, mitochondria, and synapses.

Perikaryal rind

KC perikarya surrounding the central cone of mitotic and developing cells are typically less osmophilic (Fig. 5a–c). Developing cells give rise to interdigitating extensions that are equipped with growth cone-like structures and filopodia (Figs. 5d–g, 6). These protrusions contain ribosomes, endoplasmic reticulum, microtubules, and mitochondria. Axonal fibers of mature KCs are devoid of ribosomes. The central core of sprouting KCs that enters the anterior calyx also shows irregularly shaped fibers and growth cone-like elements. Within the cup of KC perikarya, beneath its origin from newly generated perikarya and close to the level of calycal neuropil, the compact and strongly osmiophilic fiber bundle of downward-growing processes is surrounded by the electron-lucent neurites of mature KCs (Figs. 6a, 7a).

Whereas glial sheaths typically enclose somata of mature KCs (Fig. 5c), mitotic and sprouting cell bodies within the prolific cluster are not separated by glial processes. Glial projections with electron-lucent cytoplasm do, however, invade the zone of outward-growing KC fibers. These glial projections, which are resolved only by electron microscopy, are associated with other electron-dense profiles suggestive of degenerating elements (Figs. 6a–c, 7, 8) with contact to KC fibers.

Neuropil

In the anterior calyx, newly generated KC fibers of the compact core extend collaterals radially that are directed toward microglomerular neuropil (Fig. 8a–c). These fiber bundles are here identified as presumptive KC dendrites. Their minute size precluded tracing them deep into the calyx, and it is not known whether at this stage of development they participate in functional synapses. Equivalent bundles of dendrites belonging to mature KCs, however, show synaptic complexes en passant before reaching their final destinations at microglomeruli (compare synapsin-immunoreactive spots in Fig. 4c–g). Large areas filled with electron-dense material were observed within the calyx and also in deeper layers of the core region of the perikaryal rind (Figs. 7d–f, 8a–e). This osmiophilic material is interpreted as degenerating cellular debris and gives rise to minute prolongations that are accompanied by glial cytoplasm and that contact KC fibers. The processes from newly generated KCs also send out minute collaterals into this matrix. Those fibers also exhibit growth cone-like features and can be equipped with ribosomes and rough endoplasmic reticulum (Figs. 7, 8f,g).

The osmiophilic core of downward-growing fibers extends through the pedunculus and as far as the tips of the vertical and medial lobes (Figs. 9, 10). Sagittal and cross-sections of the core corroborate immunocytological observations in that core fibers are devoid of synaptic vesicles and synaptic sites. Likewise, ribosomes were not seen in core fibers except at levels within and above the calyx. The osmiophilic central core is surrounded by a ring of thin electron-lucent KC axons the diameters of which increase with distance from the core. These axons also lack synaptic organelles (Figs. 9a,b). This population of electron-lucent profiles that surrounds the osmiophilic core is itself surrounded by mature KC axons (belonging to class II KCs) that do exhibit synaptic sites with extrinsic neuron profiles (Fig. 10c). The latter often extend across bundles of KC axons, but they invade the lobe only up to the core's margin (Fig. 9). In summary, the distribution of synapses as revealed by electron microscopy corresponds to the distribution of synapsin revealed by immunocytology and confocal microscopy.

The MB's calyx, pedunculus, and lobes contain glial cytoplasmic projections that originate from glial cell bod-

Fig. 4. Differential distribution of synapsin and f-actin in mushroom bodies and circumferential neuropil; phalloidin-f-actin staining (green); antisynapsin immunolabelling (magenta). **a,b:** Central brain neuropil, overview. Note intense antisynapsin labelling in glomerular AC and in α-lobe parts (AL) and in the central body (CB). Ocellar tracts (thin arrows) show massive antisynapsin labelling but lack f-actin. Synapsin and f-actin are missing mainly in lateral pedunculus parts and in portions of the neuropil outside mushroom bodies. Strong f-actin staining of the sprouting cell cluster and central core areas (arrows); a: frontal section, magenta channel gamma = 2; b: horizontal section, magenta channel linearly stretched to saturation of 3% of all pixels. **c–g:** Antisynapsin labelling of spot-like synaptic complexes in inner parts of the AC; strong f-actin labelling of the central core area and its centrifugal projections. Synaptic complexes may or may not accompany the f-actin fascicles; horizontal sections. c–f: Seventh to tenth of consecutive optical slices (depth 0.8 μm each), the intensity histograms of which have been adjusted to the first slice of the image stack. c: Central core area with spoke-like centrifugal projections toward the glomerular layer of AC. The central core area has a fuzzy margin with numerous indentations. Note the tiny synaptic complexes in the inner parts of the calyx; horizontal section. d–f: Series of subsequent optical sections (thickness 0.8 μm) to show the extension of synaptic spots and of f-actin fascicles. g: Stereo image (7° divergence angle), maximum projections of the fourth to thirteenth slice (thickness 0.8 μm) of the same image stack with adjusted intensities. Note that this is not a magenta-green anaglyphic image; instead, the two half-images are to be fused with a stereoscopic magnifier or with naked eyes. **h:** Upper pedunculus (asterisk) with tiny synaptic spot-like areas as found in the calyx, missing in the central core area (arrow). **i:** Cross-section through basal parts of the α-lobe showing partial intense antisynapsin labelling, e.g. in peripheral parts containing fiber bundles of large Kenyon cells (asterisk) but not in the central core area (arrow). **j:** Cross-sections through β-lobe, differential antisynapsin staining of subdivisions, strong labelling of medial fiber bundles of large Kenyon cells (γ-lobe part). In the β-lobe, the f-actin-stained central core complex (arrow) is gradually shifted to the lateral margin. Scale bars = 200 μm in a,b; 20 μm in c–j.

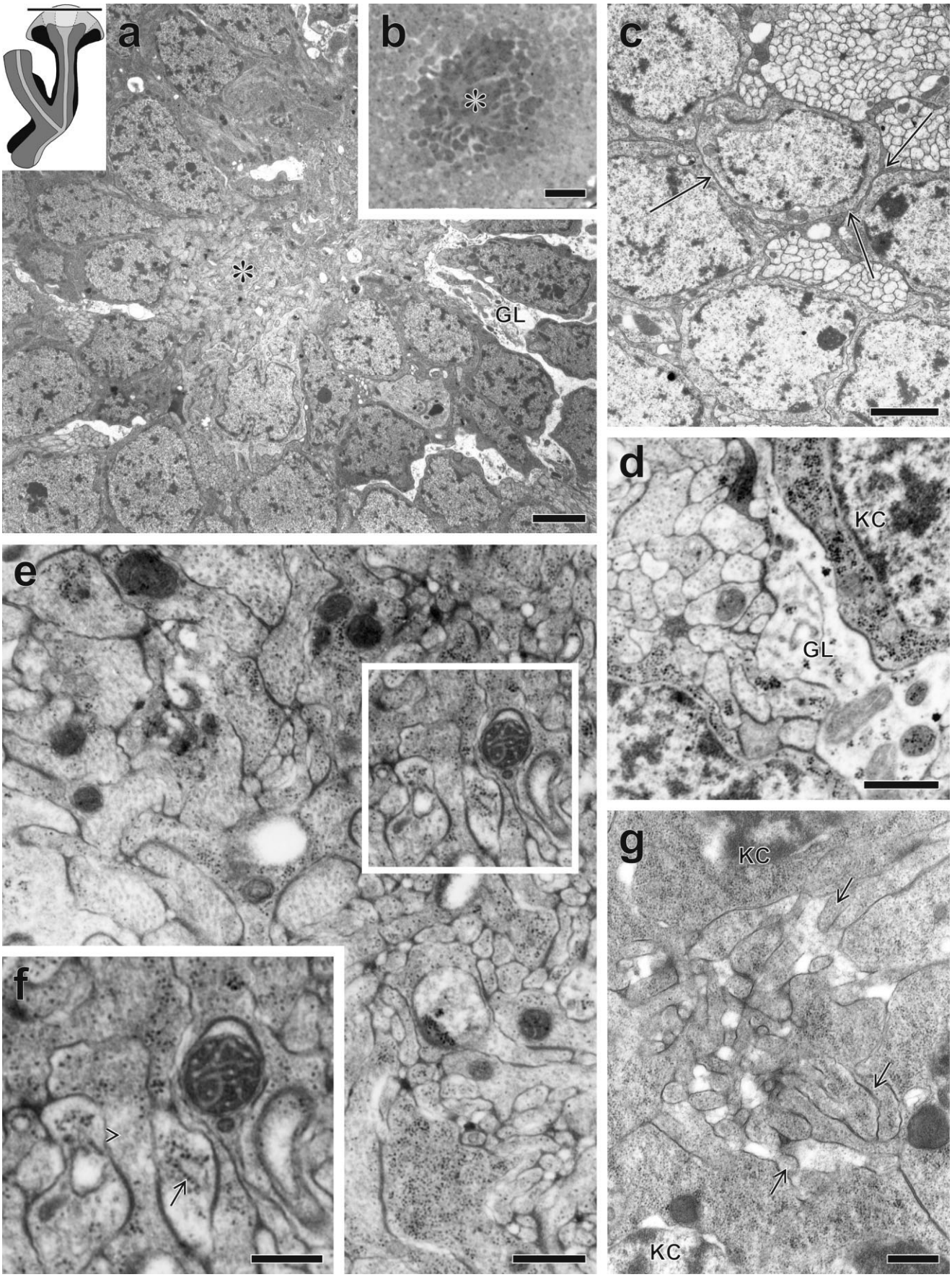

Fig. 5. Proliferating cells at the top of the perikaryal layer of Kenyon cells (KC); electron microscopy, horizontal section (see scheme for section plane). **a,b:** The cluster of mitotic and sprouting cells surrounding a central mass of interdigitating fibers (central core area; asterisk) can be discriminated by its enhanced electron density from developed KCs (see c) and glia (GL). **c:** Developed KC somata are separated by glial sheaths (arrows). **d:** Light glial cytoplasm (GL) intrudes the proliferative cluster, next to an adjacent KC. **e,f:** The central core area is filled with irregularly shaped fiber profiles of presumptive KCs. Fibers show abundant free ribosomes, rough endoplasmic reticulum (arrow), and microtubules (arrowhead). **g:** Central core with interdigitating filopodia (arrows). Scale bars = 2 μm in a,c; 5 μm in b; 0.5 μm in d,e,g; 0.3 μm in f.

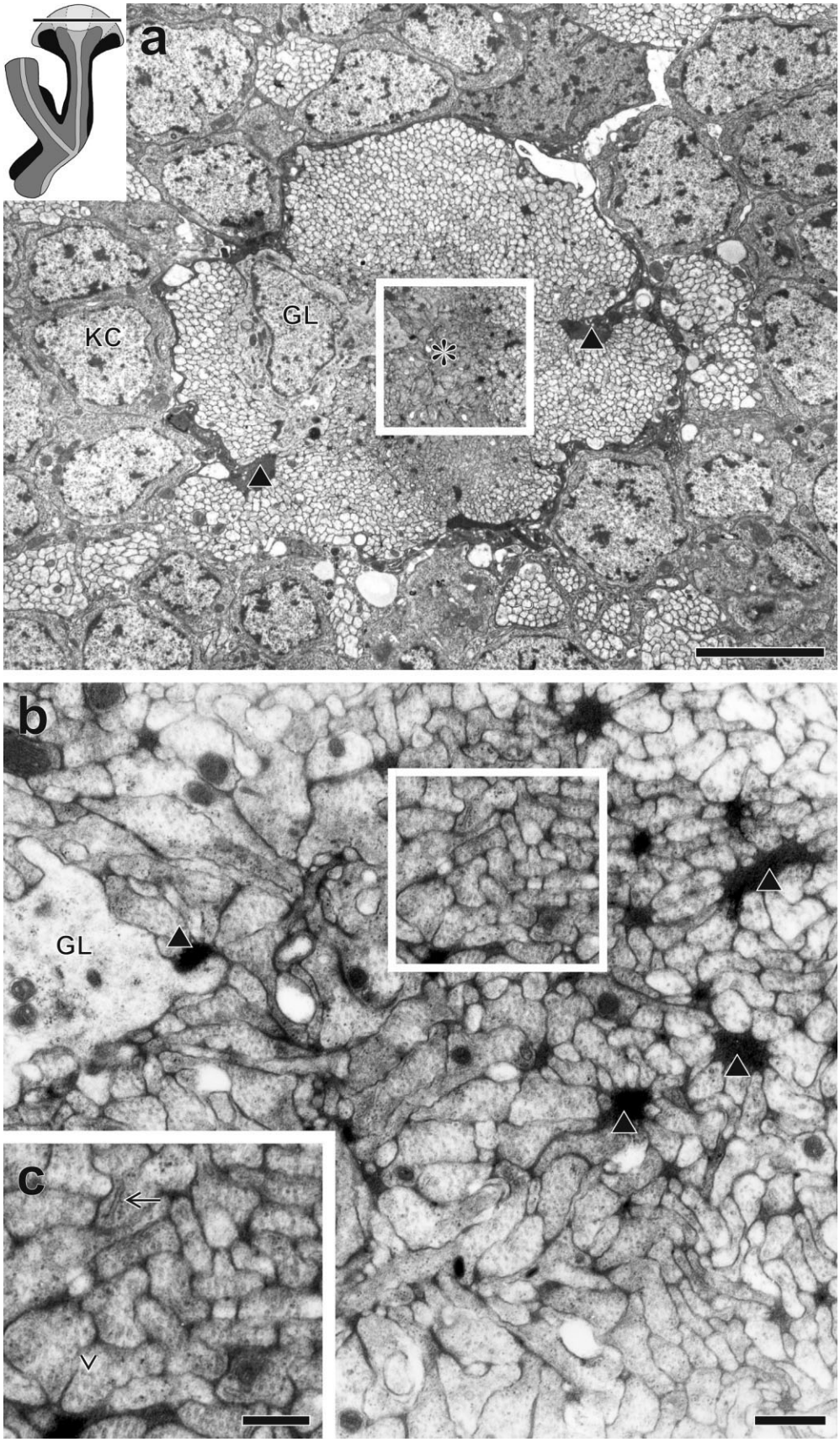

Fig. 6. Perikaryal layer of Kenyon cells (KCs) beneath the proliferative cell cluster (section level see scheme; compare Fig. 5). **a:** A mass of strongly osmiophilic sprouting fibers of the central core (asterisk) surrounded by transversely cut fiber profiles of more developed KCs descending to the calyx; a light glial cell (GL) in a marginal position of the central core. The central fiber mass is encircled and invaded by dark material of decaying cellular components (triangles). **b:** Enlarged central region as indicated in a. **c:** Further enlargement of central core as indicated in b, showing polymorphous fibers with microtubules (arrowhead). Central core polymorphous fibers with tubules (arrowhead), ribosomes, and rough endoplascmic reticulum (arrow). The electron-dense strands of decaying material (triangles) contact glial cells and neuronal fibers directly. Scale bars = 5 μm in a; 0.5 μm in b; 0.3 μm in c.

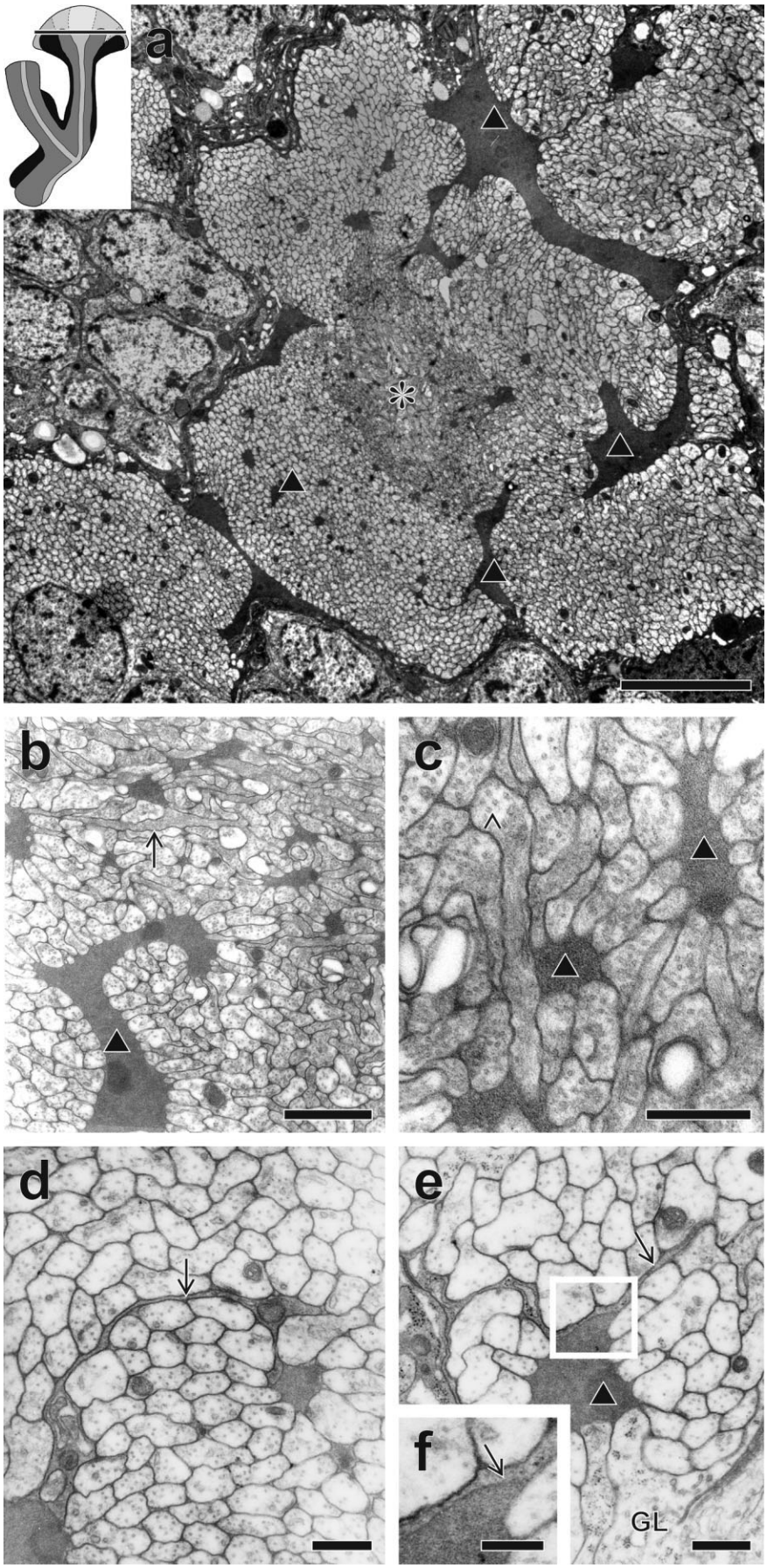

Fig. 7. Central core region at the border of the somatic layer and AC (section level see scheme). **a:** The voluminous dark areas (triangles) intrude the fiber mass of Kenyon cell axons and the central core area (asterisk). **b:** Note dark fiber profile (arrow) directed perpendicularly to the transversely cut Kenyon cell axons; decaying material (triangle). **c:** Osmiophilic collateral of a Kenyon cell axon (arrowhead); dark decaying material (triangles) surrounded by Kenyon cell fibers. **d–f:** Osmiophilic extracellular material (triangles) in direct contact to glial cytoplasm (arrows). Scale bars = 5 μm in a; 1 μm in b; 0.4 μm in c,e; 0.5 μm in d; 0.3 μm in f.

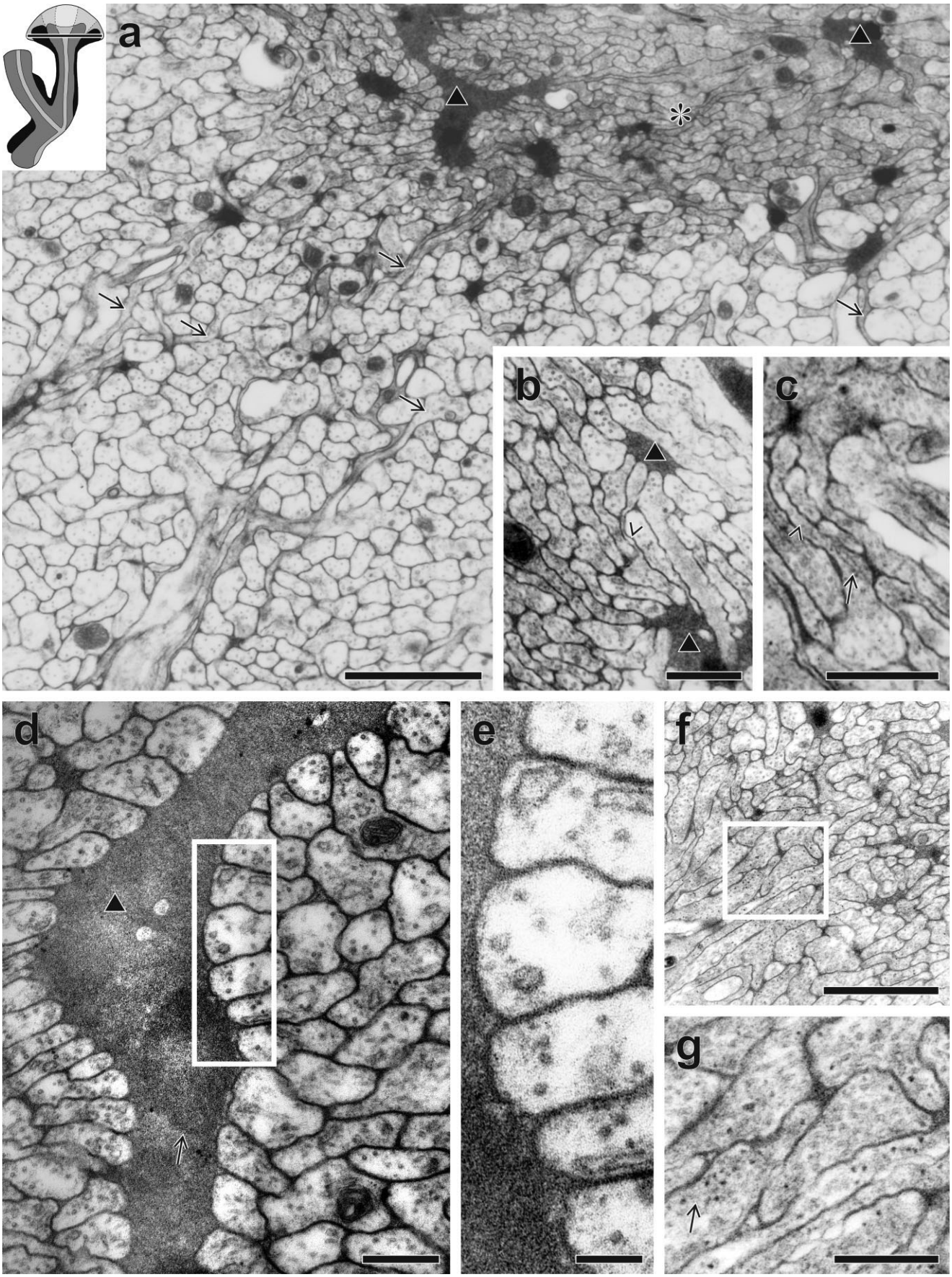

Fig. 8. Central parts of the AC in horizontal sections (section level see scheme). **a:** Central core (asterisk) with polymorphous fiber profiles holds many electron-dense compartments with degenerating material (triangles); centrifugal and centripetal fiber branches (arrows). **b,c:** Fibers with extensions (arrowheads) toward electron-dense compartments (triangles); ribosomes (arrow). **d,e:** Kenyon cell fibers adjacent to an extracellular compartment (triangle) with cellular debris (arrow). e: Note granulated contents of the extracellular space and the neighboring Kenyon cell membranes. **f,g:** Irregularly shaped fibers with ribosomes (arrow). Scale bars = 2 μm in a; 0.5 μm in b,c; 0.3 μm in d,g; 0.1 μm in e; 1 μm in f.

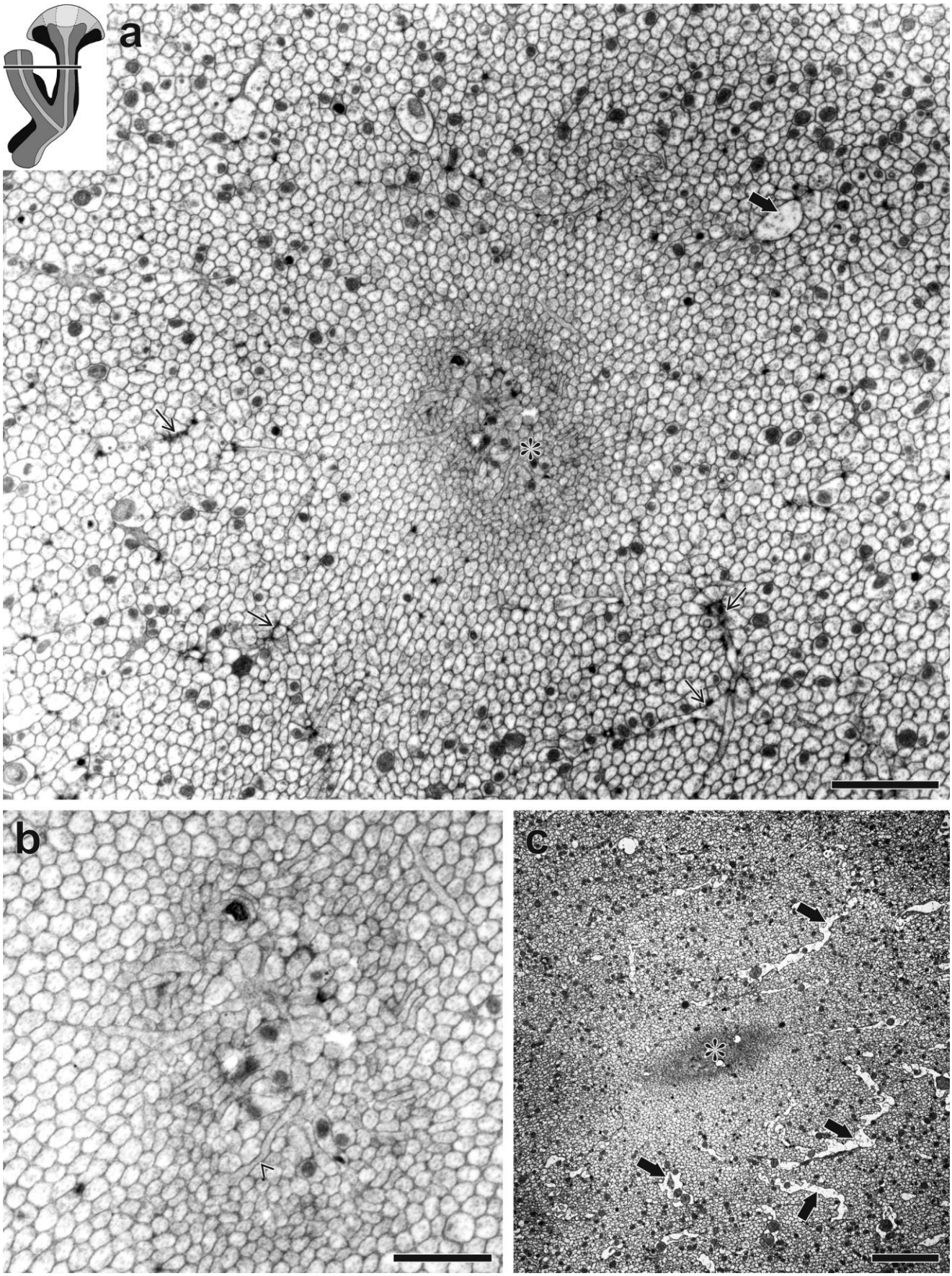

Fig. 9. Central core areas (asterisks) of α-lobe (a,b) and pedunculus (c) in cross-sections (section level see scheme). **a,b:** The innermost part of central core with polymorphous fibers gives off fiber branches. The electron density of fibers gradually decreases in a centrifugal direction, and the diameter of axonal fibers increases. A zone of light Kenyon cell fibers complexes devoid of synapses exhibits a low amount of small mitochondria. Peripheral fiber masses contain synaptic contacts (thin arrows) and extrinsic neuronal profiles (thick arrow). **c:** In the pedunculus, the central core (asterisk) is similarly encircled by tiny fibers. Extrinsic fibers (thick arrows) contact tiny Kenyon cell axons (compare Fig. 10c). Scale bars = 2 μm in a; 1 μm in b; 2 μm in c.

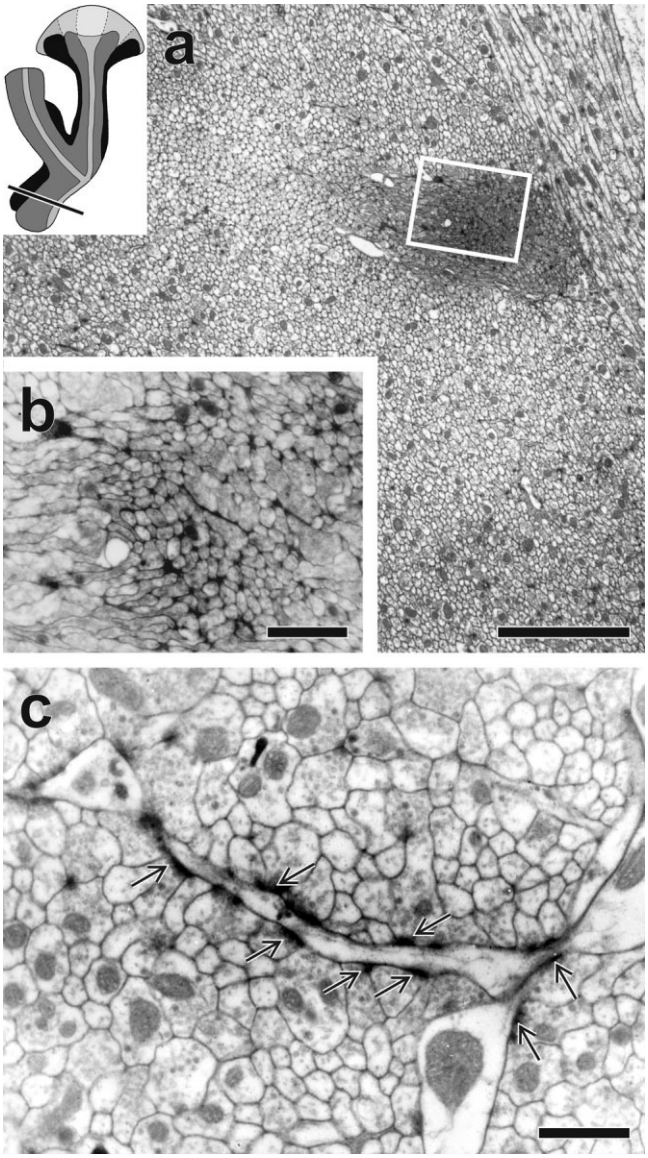

Fig. 10. **a,b:** Section through the β-lobe as indicated in the schematic **inset**. The dark central core area is shifted to the medial rim of the lobe (compare Fig. 9). The central area contains polymorphous fiber profiles and small areas with degenerating material. **c:** Fully developed Kenyon cell profiles filled with vesicles presynaptic (arrows) to a postsynaptic element. The abundance of vesicles corresponds to the intense antisynapsin labelling of α- and β-lobe parts (compare Fig. 4i,j). Scale bars = 5 μm in a; 1 μm in b,c.

ies mainly outside the MB. These glial processes provide sheathing partially around parallel subdivisions in the lobes or their corresponding zones in the calyces. Electron-dense matrix associated with a system of glial intrusions, most prominent in the anterior calyces, contains the debris of what is interpreted as degenerated cellular material. Although we could not classify this matrix into transitional stages typical of the degeneration process, we occasionally encountered in our material pycnotic KC perikarya and areas of obviously degenerating profiles (Fig. 11) but did not find massive signs of degeneration or considerable extracellular space filled with electron-dense material associated with glia. In summary, cross-sections of the stalk and lobes reveal the three concentric zones, as defined by their electron opacity and synaptic organelles: these are, from the center to periphery, the dark central core, its surround of small-diameter KC axons lacking synapses, and around this mature class II and III KC axons that contribute to synaptic interactions with invading extrinsic neurons.

Distribution of organelles

Both light microscopy and electron microscopy of MBs suggest dynamic growth processes associated with core fibers and the central cohort of newly generated cell bodies above the anterior calyx. To substantiate these qualitative observations, diameters of fibers and their equipment with organelles were assessed systematically from large EM montages collected from different levels of the calyx, stalk, and lobes (Figs. 12, 13). In the stalk, profile cross-sections appear irregularly shaped in the central core, often forming small protrusions interpreted here as sectioned growth cones. The very smallest fiber profiles at the core center have diameters of about 0.15 μm. From the central core outward, fiber diameters progressively increase. The largest that participate in synaptic connections correspond to class II KC fibers, and these are clearly separated from the cohort of even larger class III KC axons that will contribute to the γ-division of the lobes. The number of microtubules within the axons also relates to fiber area (Fig. 12a). Data points represent means from test squares of identical sizes. Their coefficients of variation are quite similar, ranging between 0.097 and 0.136 for fiber area and between 0.096 and 0.107 for number of tubuli. The quotient of mean microtubule number and mean fiber area (Fig. 12b) varies from center to periphery in a somewhat complex manner. It shows a first minimum next to the KC I to KC II transition, increases progressively outward within the ensemble of class II KC axons ring, and decreases to a final minimum at the boundary between the class II and class III KC axons.

In the lobes, there is a similar increase of KC fiber diameter from the center outward. The lobes are wider compared with the stalk, because Kenyon cell fibers are equipped with blebs and short lateral projections, and there is a substantial contribution to the lobes by the terminals and dendrites of extrinsic fibers. The numbers of synapses (for definition and forms of chemical synapses in insects see Watson and Schürmann, 2002) and mitochondria (Fig. 13) were counted in electron micrographs from different section levels of calyx, stalk, and lobes as indicated. Synapse number increases toward centrifugal neuropil portions.

As in the pedunculus, the core is devoid of synapses. Synapse density increases outward among KC axons, representing different birth dates. However, the situation is made somewhat more complicated in that, farthest from the core, there are relatively few synapses (Fig. 13). This is because the KC axons are "diluted" by the presence of large profiles belonging to incoming and outgoing extrinsic arborizations. Likewise, the incidence of mitochondria roughly parallels the distribution of synapses.

In summary, observations of MB ultrastructure confirm and elaborate on the confocal observations described above. Newly generated KCs in adult brains undergo progressive structural modifications to become fully matured

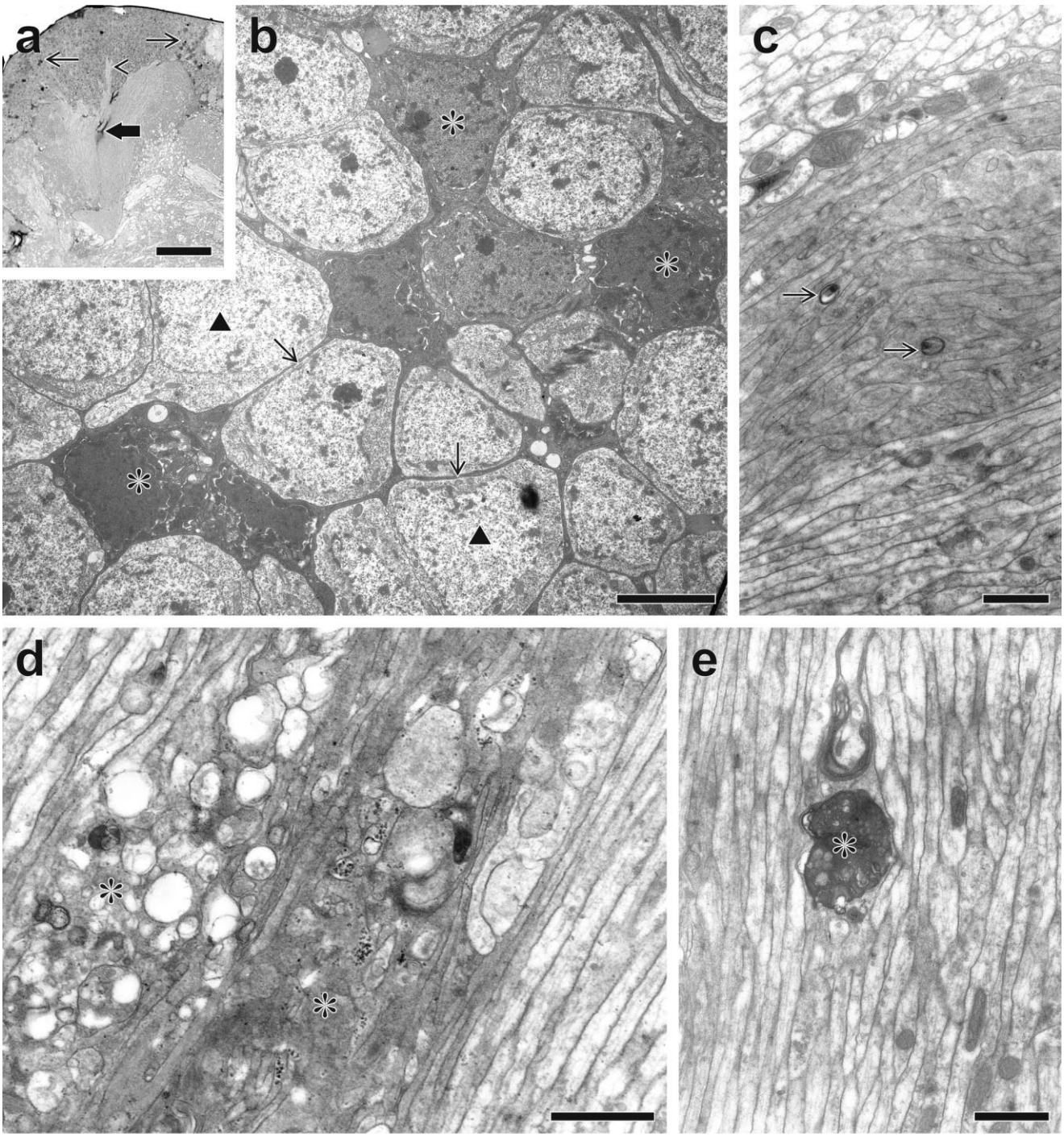

Fig. 11. Degeneration in the mushroom bodies indicated by osmiophilic reaction of cellular material; a: light microscopy; b–e: electron microscopy. **a:** Some pycnotic KC somata (arrows); note osmiophilic patches (thick arrow) in the AC adjacent to the central core sprouting fiber mass (arrowhead). **b:** Degenerating Kenyon cell somata (asterisks) and intact neuronal perikarya (triangles) separated by glial sheaths (arrows); horizontal section. **c:** Degenerating elements (arrows) within the dark central core fiber complex lacking mitochondria; AC, sagittal section. **d,e:** Different aspects of degeneration (asterisks) at the rim of the central core; pedunculus, sagittal section. Scale bars = 20 μm in a; 2 μm in b; 1 μm in c–e.

KC neurons equipped with synaptic specializations. In the course of this maturation process, new KCs form dendrites in the anterior calyx, and new axons become displaced outward away from the center of the core to become integrated into cohorts of mature axons. The dynamics of growth, development, and synaptic integration are re-

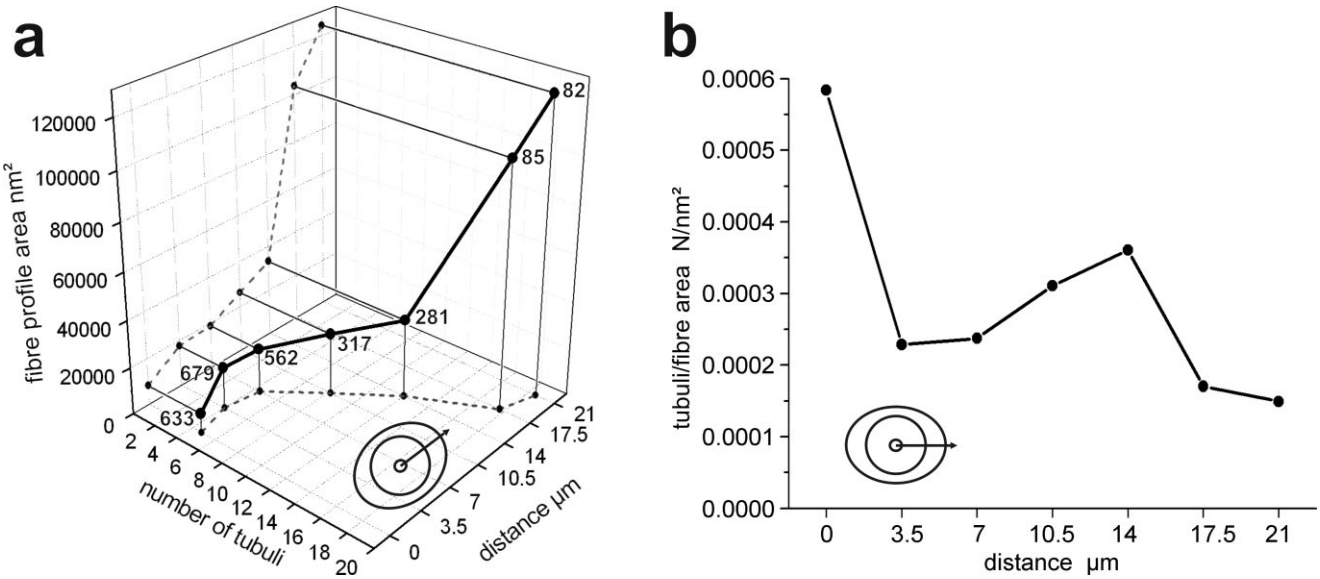

Fig. 12. Mean fiber area of Kenyon cells and number of microtubules per fiber depend on position within the pedunculus. Starting at the pedunculus's center, data were measured in neighbouring fields along the major axis of the elliptic borderline of the pedunculus (schematic drawing). **a:** Both parameters increase in a nonlinear manner with distance from the center, with the largest change of fiber area next to the periphery (projection to left vertical plane) and a fast rise of tubule number in the middle ring (projection to bottom plane). This results in a winding curve between data points in 3D parameter space. Numbers of Kenyon cells per test field are indicated next to data points, which represent means of one square field each. **b:** The relation of tubule number per fiber area yields a measure to define the border between center, middle ring, and periphery of the cross-sectioned pedunculus, which are hard to separate otherwise (compare Fig. 9). The curve falls sharply at both the inner and the outer margin of the middle ring but rises within this ring.

flected by the form, distribution, and complements of organelles.

DISCUSSION

In larval and adult crickets, a cone-like ensemble of neuroblasts, located midway above the anterior calyx, continues to generate new KCs, the processes of which grow down into the pedunculus and lobes to provide a discrete core of immature fibers. Cellular and subcellular features of sprouting KCs in the central core differ from those of surrounding mature KCs.

We will focus the discussion on the following points: 1) comparison of juvenile and adult forms of different species with sprouting KCs in core-like ensembles marked by phalloidin-f-actin and other molecules; 2) subcellular neuronal and glial features in growing neuropils indicating structural dynamics and transition; 3) morphological aspects of the status of sprouting KCs in the functional synaptic network of the MBs; and 4) revision of a previous classification of KCs in adult crickets.

The core of sprouting Kenyon cells

We have shown that mitotic and proliferative cell bodies of KCs are disposed as a cone-shaped cluster at the center of the dense mass of KC perikarya that overlies the anterior calyx. This cohort of neuroblasts can be identified both in larval and in adult brains of *Gryllus bimaculatus* by its affinity to antiphosphohistone immunolabelling. Among the cohort of newly generated KC somata, previously described in cricket MBs from BrdU staining, the oldest are farther away from the region of mitosis (Cayre et al., 2000; Malaterre et al., 2002).

Their outward-growing fibers form a compact central core intensely labelled by fluorescent phalloidin. Phalloidin-f-actin occurs in the tips of growth cones clearly demonstrated in insect cell culture (Tucker et al., 2004). High f-actin contents in compact fiber bundles have been similarly found in sprouting KC proliferation centers of immature larval and nymphal forms of different species (Kurusu et al., 2002; Farris and Sinakevitch, 2003; Farris et al., 2004), reflecting fiber growth and potential motility. In larval *Drosophila*, the sprouting central core fibers express fasciclin II, essential for their proper growth and organization of KCs, and can therefore be distinguished from surrounding developed KC axons (Kurusu et al, 2002). A recent study by Maynard et al. (2007) shows the distribution of the protein semaphorin 2a in adult MBs of the cricket *Gryllus bimaculatus*. Semaphorin is involved in axonal and dendritic guidance of developing neurons. There is an intense semaphorin-like immunolabelling of KC somata entouring the small, peripheral, unstained conus where mitotic activity takes place, and stained neuropil of calyx and pedunculus surrounds the unstained central core cylinder. The authors discuss their findings in the context of synapse formation and synaptic suppression. A suppression of synapse formation, mediated by semaphorin secretion, would fit with our observation on the lack of synapses in the central core column.

Addition and integration of newly formed KCs would require continuous remodelling in the calyces and other MB parts of adult crickets also involving extrinsic neurons. Dendritic growth and remodelling have been previously described in *Drosophila* KCs with the use of molecular genetic techniques (Zhu et al., 2003) and by morphological analysis of KCs through pupal and imagi-

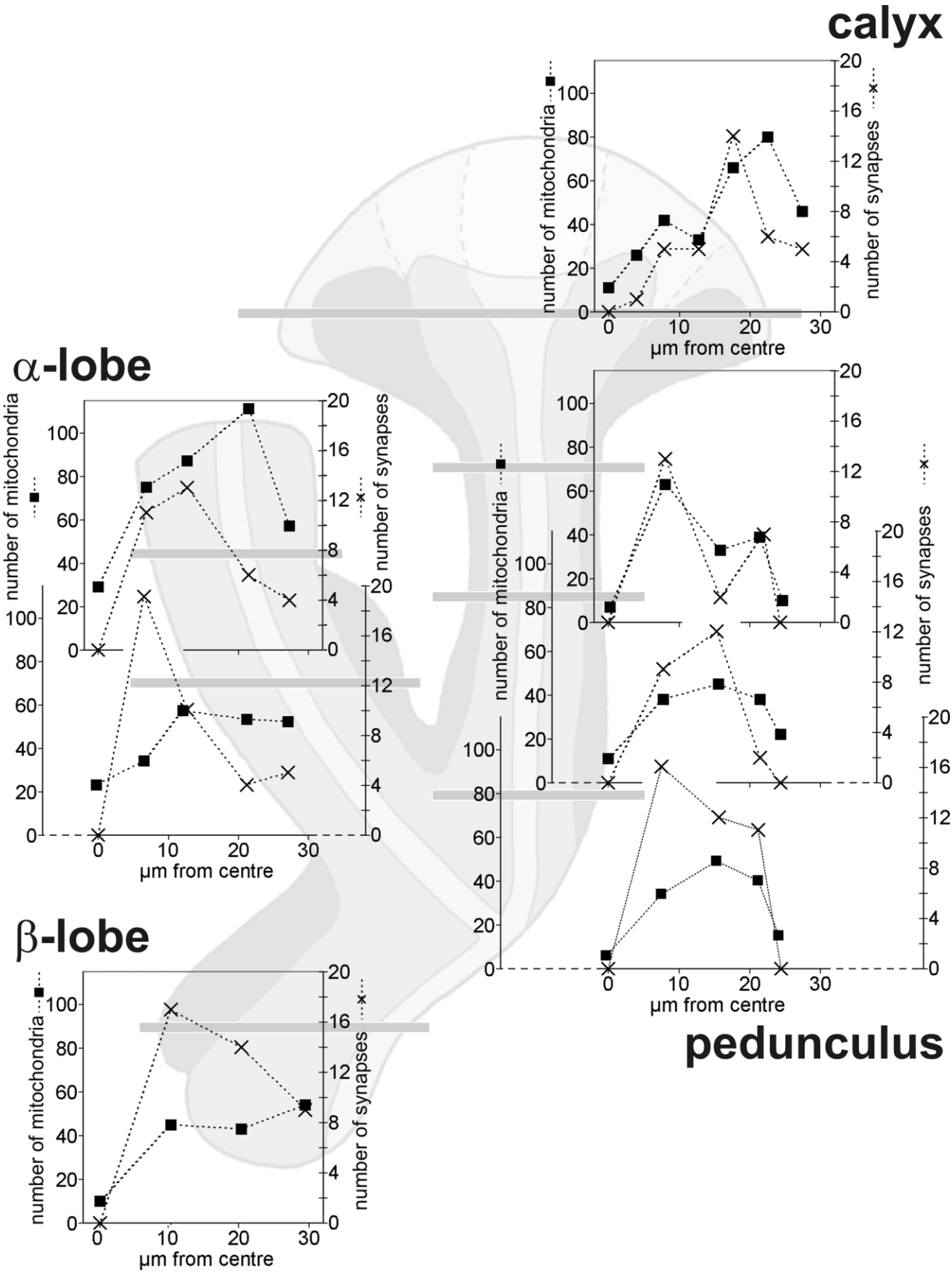

Fig. 13. Distribution of synapses and mitochondria in the mushroom body neuropil; counts from thin section samples taken at different levels (horizontal gray lines in the scheme corresponding to overlayed coordinate systems). The samples represent montages of 3 × 3-μm^2 squares aligned centrifugally from the sprouting core of Kenyon cell fibers (white areas in the cylinder-like pedunculus and lobes) to the areas with developed Kenyon cell fibers at one side of the pedunculus and lobes. At all levels, the tendency to increase the numbers of synapses and mitochondria centrifugally from the sprouting area is observed. This reflects growth and functional integration of Kenyon cell fibers.

nal development of honey bees (Farris and Strausfeld, 2001). Structural plasticity in adult MBs of species devoid of adult neurogenesis has been found in the appearance of new postsynaptic spines of KC dendrites, enlargment of extrinsic presynaptic boutons, and MB volume changes (Durst et al., 1994; Gronenberg et al., 1996; Farris et al., 2001; Seid et al., 2005).

We detected phalloidin-f-actin labelling of patches and stripes outside the compact, strongly labelled central core in all neuropil portions containing synapsin and synaptic sites. These observations might indicate structural plasticity of developed neurons, also reported for presynaptic boutons and dendritic spines of vertebrate nervous systems (Dillon and Goda, 2005).

Ultrastructural characters of developing Kenyon cells

There have been relatively few studies of fine structural changes during neurogenesis in embryonic, larval, and adult central nervous systems of insects (for review see Meinertzhagen, 2001). They have focussed on the optic lobes (Meinertzhagen, 2001), antennal lobes (Salecker and Boeckh, 1995; Acebes and Ferrus, 2001; Brown et al., 2002; Devaud et al., 2003), and MBs of *Drosophila* (Technau and Heisenberg, 1982; Technau, 1984). The most detailed was that by Salecker and Boeckh (1995) describing successive modifications of labelled neurons in the antennal lobes. Here we were able to relate the distribution of fluorescent phalloidin-f-actin labelling in confocal sections with areas of high electron density in specific cell profiles, using conventional osmic acid fixation. This has allowed the identification of sprouting outgrowths from newly generated KC bodies and their downward-growing axons. However, we cannot exclude the possibility that the concentric zone of small-diameter and electron-lucent axons also expresses phalloidin-f-actin staining as well. These axons belong to KCs on their way to becoming mature.

The central core of sprouting cells is set off against surrounding older neurons by its strong electron density. Enhanced cytoplasmic electron density either is found in sprouting neural and glial cells (this study; Salecker and Boeckh, 1995) or represents decaying degenerating material in these cell types (Schürmann, 1987; Watts et al., 2003, 2004; Brown and Strausfeld, 2006). The glial system has been demonstrated to be crucially involved in growth processes sorting the neuropil into subdivisions and to serve for intimate contact with nerve cells (Tolbert and Oland, 1990; Rössler et al., 1999; Tucker et al., 2004). Our ultrastructural data on the KC perikaryal layer also show that areas just peripheral to the core of inward-growing KC axons reveal an electron-dense matrix with interspersed glial cell extensions.

Degenerating material in our study represents only a minority compared with bundles of intact through-running parallel KC fibers. This and the absence of abundant pycnotic KCs has been similarly noted for KCs of the house cricket (Cayre et al., 2005). In adult cricket brains, space required during addition of newly generated KCs is not produced by elimination of existing neurons, which is different from the situation noted for transient KCs in pupal stages of bees (Ganeshina et al., 2000). Instead, neurogenesis in adult cricket MBs contributes to an increase of MB volume (compare Scotto-Lomassese et al., 2003).

In adult crickets, small amounts of extracellular space partially invaded by growth cone-like extensions were found only in the perikaryal layer and in the inner parts of calyx central core. In contrast, the extracellular space in antennal lobe neuropil of the cockroach embryo is invaded and sequentially filled by freely extending growth cones and filopodia of growing fibers, contacting each other and, in later stages, forming polarized synapses in structured glomeruli (Salecker and Boeckh, 1995). We consider irregularly shaped fiber profiles gathered in the central core of cricket MBs to be growth cones. This central package of sprouting fibers should deliver the driving force for a centrifugal shift of more developed fibers in concentric arrangement, also previously proposed for preimaginal stages of development for hemi- and holometabolic insects (Cayre et al., 2000; Kurusu et al., 2002; Farris and Sinakevitch, 2003).

An interesting feature is the presence of abundant ribosomes and rough endoplasmic reticulum only in sprouting fibers of the central core, but not in mature KCs or in their dendritic arborizations. In the mature insect nervous systems, neuronal RNA and ribosomes are generally confined to the perikaryal layer (Schürmann, 1987), whereas free ribosomes and rough endoplasmic reticulum have been observed in neuronal and glial growth cones, in filopodia (Tolbert and Oland, 1990) and other large neuronal processes in embryonic neuropil (Salecker and Boeckh, 1995) as well as in growing neuromuscular junctions (Rheuben et al., 1999). Our findings of such subcellular components within core fibers therefore reveal persisting embryonic features within an adult neuropil.

Further evidence that development persists throughout adult life is suggested by fiber measurements and counts of organelles in representative sections of the calyx, peduncullus, and lobes. These clearly show a differential distribution from the center of the core outward that relates to age.

Structure of sprouting KCs and functional integration

A question is whether activity found in fully developed KCs may be influenced by newly generated fibers of the central core and adjacent surrounding tiny KC axons. The presence of synapses and transmitters/neuromodulators may point to synaptic activity or its preparation in newly formed neurons.

Evidence that the core of newly generated KC fibers does not participate in synaptic integration comes not only from the failure of immunolabelling to detect synapsin or synapses by electron microscopy in the core fibers but also from the complete absence of γ-aminobutyric acid (GABA)-ergic elements in the core. GABA is found exclusively in extrinsic neurons. Small GABA-like fibers, belonging to the vast GABAergic system in all compartments of MB neuropil, end at the margin of the central core of the pedunculus and the lobes (Strambi et al., 1998; Schürmann et al., 2000) but never invade it. GABA receptors are also absent from the phalloidin-positive core (Strambi et al., 1998).

Putative transmitters and neuropeptides shown in segregated classes of intrinsic MB KCs by histochemical and immunocytological studies (Schürmann, 1987; Schürmann and Erber, 1990; Bicker, 1999; Strausfeld et al., 2000; Sinakevitch et al., 2001; Nässel and Homberg, 2006) may be expressed in the central core. Downward-growing

axons of newly generated KCs in the cricket (Schürmann et al., 2000) and in the cockroach (Sinakevitch et al., 2001; Farris and Sinakevitch, 2003; Strausfeld et al., 2003) express glutamate, proposed as a putative transmitter (Xia et al., 2005). There is, however, still no experimental proof of the transmitter status of glutamate in MBs.

For interaction of mature KCs and central core elements gaseous nitric oxide (NO) indicated for KCs (Schürmann, 2000; Cayre et al., 2005) must be taken into account. Cayre et al. (2005) have recently presented evidence for NO generated in cricket KCs, shown by in situ hybridization of NO synthase-RNA in KC perikarya surrounding, but lacking in the sprouting cells. NO synthase is produced not in sprouting KCs or in central core fibers but in surrounding more mature KCs and in the large KCs. NO could diffuse into the central core column. A recent study on grasshopper MBs (Ott et al., 2007) gives good evidence for NO diffusion from so-called KC fiber tubules to inner KC fiber bundles devoid of NO, indicating interaction between KC neuropil subdivisions. We conclude that the young central core KC fibers do not participate directly in synaptic signalling but may receive NO signal transfer before expressing morphological synapses.

Classification of KCs

Three discrete, nonisomorphic classes of morphologically distinct KCs have previously been distinguished in cricket MBs (Schürmann, 1973). These classes occupy separate MB subdivisions. Class III KCs form the γ-lobe portion of the β-lobe (for terminology compare Strausfeld, 2002). These KCs are all generated before imaginal hatching and represent the oldest group of KCs (Lee et al., 1999; Malaterre et al., 2002; Farris and Sinakevitch, 2003; Mizunami et al., 2004). It is noteworthy that class III neurons that contribute to the γ-divisions of the lobes are not augmented in adults by newly formed intrinsic KCs. Class I and II KCs of the anterior perikaryal rind form dendrites in the anterior calyx. The former type I KC with short dendrites and few spines and sparsely equipped with axonic blebs and collaterals had been set apart from type II KC. From our light and electron microscopic findings, we revise the classification of KC I and II types deduced from Golgi impregnations (Schürmann, 1973). We now regard class I neurons to be the maturing precursors of more elaborate class II cells. Categorization of KCs can be accorded only to mature neurons in the cricket and in other species (Strausfeld et al., 1998, 2003; Farris and Sinakevitch, 2003; for review see Fahrbach, 2006).

The central core is characterized by lack of extrinsic fibers invading it; the absence of chemical synapses; the absence of dendrites from it in the anterior calyx; and the fact that, except for the mysterious role of glutamate, no putative transmitter candidates can at present be attributed to it. From the available data, the core of developing KCs must be viewed as representing transient morphologies.

ACKNOWLEDGMENTS

We thank Dr. E. Buchner (Würzburg, Germany) and Dr. A. Hofbauer (Regensburg, Germany) for the gift of antibodies, and Mrs. Marion Knierim-Grenzebach (now Fort Knox, KY) for skillfull technical assistance. We owe special thanks to Dr. N. Strausfeld (Tucson, AZ) for critically reading a previous version of the manuscript and for his very helpful suggestions. The English text has been corrected by M. Locke (Göttingen, Germany).

LITERATURE CITED

Acebes A, Ferrus A. 2001. Increasing the number of synapses modifies olfactory perception in *Drosophila*. J Neurosci 21:6264–6273.

Bicker G. 1999. Histochemistry of classical neurotransmitters in antennal lobes and mushroom bodies of the honeybee. Microsc Res Techniq 45:174–183.

Bieber M, Fuldner D. 1979. Brain growth during adult stage of a holometabolous insect. Naturwissenschaften 66:426.

Brown SM, Strausfeld NJ. 2006. Development-dependent and -independent ubiquitin expression in divisions of the cockroach mushroom body. J Comp Neurol 496:556–571.

Brown SM, Napper RM, Thompson CM, Mercer AR. 2002. Stereological analysis reveals striking differences in the structural plasticity of two readily identifiable glomeruli in the antennal lobes of the adult worker honeybee. J Neurosci 22:8514–8522.

Cayre M, Strambi C, Charpin P, Augier R, Meyer MR, Edwards JS, Strambi A. 1996. Neurogenesis in adult insect mushroom bodies. J Comp Neurol 371:300–310.

Cayre M, Malaterre J, Charpin P, Strambi C, Strambi A. 2000. Fate of neuroblast progeny during postembryonic development of mushroom bodies in the house cricket, *Acheta domesticus*. J Insect Physiol 46:313–319.

Cayre M, Malaterre J, Scotto-Lomassese S, Strambi C, Strambi A. 2002. The common properties of neurogenesis in the adult brain: from invertebrates to vertebrates. Comp Biochem Physiol B132:1–15.

Cayre M, Malaterre J, Scotto-Lomassese S, Holstein GR, Martinelli GP, Forni C, Nicolas S, Aouane A, Strambi C, Strambi A. 2005. A role for nitric oxide in sensory induced neurogenesis in an adult insect brain. Eur J Neurosci 21:2893–2902.

Devaud JM, Acebes A, Ramaswami M, Ferus A. 2003. Structural and functional changes in the olfactory pathway of adult *Drosophila* take place at a critical age. J Neurobiol 56:13–23.

Dillon C, Goda J. 2005. The actin cytoskeleton: integrating form and function at the synapse. Annu Rev Neurosci 28:25–55.

Dufour MC, Gadenne C. 2006. Adult neurogenesis in a moth brain. J Comp Neurol 495:635–643.

Durst C, Eichmüller S, Menzel R. 1994. Development and experience lead to increased volume of subcompartments of the honeybee mushroom body. Behav Neural Biol 62:259–263.

Erber J, Homberg U, Gronenberg W. 1987. Functional roles of the mushroom bodies in insects. In: Gupta P, editor. Arthropod brain: its evolution, development, structure, and functions. New York: John Wiley & Sons. p 485–511.

Fabian-Fine R, Volknandt W, Seyfarth E. 1999. Peripheral synapses at identifiable mechanosensory neurons in the spider *Cupiennius salei*: synapsin-like immunoreactivity. Cell Tissue Res 295:13–19.

Fahrbach SE. 2006. Structure of the mushroom bodies of the insect brain. Annu Rev Entomol 51:209–232.

Farris SM, Sinakevitch I. 2003. Development and evolution of the insect mushroom bodies: towards the understanding of conserved developmental mechanisms in a higher brain center. Arthropod Struct Dev 32:79–101.

Farris SM, Strausfeld NJ. 2001. Development of laminar organization on the mushroom bodies of the cockroach: Kenyon cell proliferation, outgrowth, and maturation. J Comp Neurol 439:331–351.

Farris SM, Robinson GE, Fahrbach SE. 2001. Experience- and age-related outgrowth of intrinsic neurons in the mushroom bodies of the adult worker honey bee. J Neurosci 21:6395–6404.

Farris SM, Adams A, Strausfeld NJ. 2004. Development and morphology of class II Kenyon cells in the mushroom bodies of the honey bee, *Apis mellifera*. J Comp Neurol 474:325–339.

Frambach I, Rössler W, Winkler M, Schürmann F-W. 2004. F-actin at identified synapses in the mushroom bodies of the insect brain. J Comp Neurol 475:303–314.

Ganeshina O, Schäfer S, Malun D. 2000. Proliferation and programmed cell death of neuronal precursors in the mushroom bodies of the honey bee. J Comp Neurol 417:349–365.

Godenschwege T, Reisch D, Diegelmann S, Eberle K, Funk, N, Heisenberg M, Hoppe V, Hoppe J, Klagges BRE, Martin R-N, Nikitina EA, Putz G,

Reifengerste R, Reisch N, Rister J, Schaupp M, Scholz H, Schwärzel M, Werner U, Zars ZD, Buchner S, Buchner E. 2004. Flies lacking all synapsins are unexpectedly healthy but are impaired in complex behaviour. Eur J Neurosci 20:611–622.

Gould E, Gross CG. 2002. Neurogenesis in adult mammals: some progress and problems. J Neurosci 22:619–623.

Groh C, Tautz J, Rössler W. 2004. Synaptic organization in the adult honey bee brain is influenced by brood-temperature control during pupal development. Proc Nat Acad Sci U S A 101:4268–4273.

Groh C, Ahrens D, Rössler W. 2006. Environment- and age-dependent plasticity of synaptic complexes in the mushroom bodies of honey bee queens. Brain Behav Evol 68:1–14.

Gronenberg W, Heeren S, Hölldobler B. 1996. Age-dependent and task-related morphological changes in the brain and the mushroom bodies of the ant, *Camponotus floridanus*. J Exp Biol 119:2011–2019.

Harzsch S, Anger K, Dawirs RR. 1997. Immunocytochemical detection of acetylated alpha-tubulin and *Drosophila* synapsin in the embryonic crustacean nervous system. Int J Dev Biol 41:477–484.

Harzsch S, Miller J, Benton J, Beltz B. 1999. From embryo to adult: persistent neurogenesis and apoptotic cell death shape the lobster deutocerebrum. J Neurosci 19:3472–3485.

Heisenberg M. 2003. Mushroom bodies memoir: from maps to models. Nat Rev Neurosci 4:266–275.

Hendzel MJ, Wei Y, Manzini MA, Van Hooser A, Ranalli T, Brinkley BR, Bazett-Jones, Allis CD. 1997. Mitosis-specific phosphorylation of histone H3 initiates primarily with pericentromeric heterochromatin during G2 and spreads in an ordered fashion coincident with mitotic chromosome condensation. Chromosoma 106:348–360.

Huber F. 1960. Untersuchungen über die Funktion des Zentralnervensystems und insbesondere des Gehirns bei der Fortbewegung und der Lauterzeugung der Grillen. Z Vergl Physiol 44:60–132.

Klagges BRE, Heimbeck G, Godenschwege TA, Hofbauer A, Pflugfelder GO, Reifegerste R, Reisch D, Schaupp M, Buchner S, Buchner E. 1996. Invertebrate synapsins: a single gene codes for several isoforms in *Drosophila*. J Neurosci 16:3154–3165.

Kurusu M, Awasaki T, Masuda-Nakagawa LM, Kawauchi H, Ito K, Furukubo-Tokunaga K. 2002. Embryonic and larval developmenet of the *Drosophila* mushroom bodies: concentric layer subdivisions and the role of fasciclin II. Development 129:409–419.

Le Dizet M, Piperno G. 1987. Identification of an acetylation site of *Chlamydomonas* α-tubulin. Proc Natl Acad Sci U S A 84:5720–5724.

Lee T, Lee A, Luo L. 1999. Development of the *Drosophila* mushroom bodies: sequential generation of three distinct types of neurons from a neuroblast. Development 126:4065–4076.

Leitinger G, Pabst MA, Rind FC, Simmons PJ. 2004. Differential expression of synapsin in visual neurons of the locust *Schistocerca gregaria*. J Comp Neurol 480:89–100.

Malaterre J, Strambi C, Aouane A, Strambi A, Cayre M. 2002. Development of cricket mushroom bodies. J Comp Neurol 452:215–227.

Malun D, Moseleit AD, Grünewald B. 2003. 20-Hydroxyecdysone inhibits the mitotic activity of neuronal precursors in the developing mushroom bodies of the honey bee, *Apis mellifera*. J Neurobiol 57:1–14.

Martini SR, Davis RL. 2005. The dachshund gene is required for the proper guidance and branching of mushroom body axons in *Drosophila melanogaster*. J Neurobiol 64:133–144.

Mashaly A, Schürmann F-W, Frambach I. 2003. A substrate for plasticity: Sprouting neurons in an olfactory neuropile of the mature cricket brain. Comp Biochem Physiol 134A:S67–S68.

Matus A. 1999. Postsynaptic actin and neuronal plasticity. Curr Opin Neurobiol 9:561–565.

Maynard KR, McCarthy SS, Sheldon E, Horch HW. 2007. Development and adult expression of semaphorin 2a in the cricket *Gryllus bimaculatus*. J Comp Neurol 503:169–181.

Meinertzhagen IA. 2001. Plasticity in the insect nervous system. Adv Insect Physiol 28:84–167.

Menzel R. 2001. Searching for the memory trace in a mini-brain, the honeybee. Learn Mem 8:53–62.

Mizunami M, Yokohari F, Takahata M. 2004. Further exploration into the adaptive design of the arthropod "microbrain": sensory and memory-processing systems. Zool Sci 21:1141–1151.

Nässel DR, Homberg U. 2006. Neuropeptides in interneurons of the insect brain. Cell Tissue Res 326:1–24.

Okada R, Rybak J, Manz G, Menzel R. 2007. Learning-related plasticity in PE1 and other mushroom body extrinsic neurons. J Neurosci 27: 11736–11747.

Ott SR, Philippides A, Elphick MR, O'Shea M. 2007. Enhanced fidelity of diffusive nitric oxide signalling by the spatial segregation of source and target neurons in the memory centre of an insect brain. Eur J Neurosci 25:181–190.

Panov AA. 1957. The structure of the brain in insects in successive stages of postembryonic development. Entomol Rev U S S R 36:269–284.

Pascual A, Preat T. 2001. Localization of long term memory within the *Drosophila* mushroom body. Science 294:1115–1117.

Rheuben MB, Yoshihara M, Kidokoro Y. 1999. Ultrastructural correlates of neuromuscular junction development. Int Rev Neurobiol 43:69–92.

Robinson DG, Ehlers U, Herken R, Herrmann B, Mayer F, Schürmann F-W. 1987. Methods of preparation for electron microscopy. Berlin: Springer.

Rossbach W. 1962. Histologische Untersuchungen über die Hirne naheverwandter Rüsselkäfer (Curculionidae) mit unterschiedlichem Brutfürsorgeverhalten. Z Morphol Ökol Tiere 50:616–650.

Rössler W, Oland LA, Higgins MR, Hildebrand JG, Tolbert LP. 1999. Development of a glia-rich axon-sorting zone in the olfactory pathway of the moth *Manduca sexta*. J Neurosci 19:9865–9877.

Rössler W, Kuduz J, Schürmann F-W, Schild D. 2002. Aggregation of f-actin in olfactory glomeruli: a common feature of glomeruli across phyla. Chem Senses 27:803–810.

Salecker I, Boeckh J. 1995. Embryonic development of the antennal lobes of a hemimetabolous insect, the cockroach *Periplaneta americana*: light and electron microscopic observations. J Comp Neurol 352:33–54.

Scharff C. 2000. Chasing fate and function of new neurons in adult brains. Curr Opin Neurobiol 10:774–783.

Schürmann F-W. 1972. Über die Struktur der Pilzkörper des Insektenhirns II. Synaptische Schaltungen im Alpha-Lobus des Heimchens *Acheta domesticus* L. Z Zellforsch 127:240–257.

Schürmann F-W. 1973. Über die Struktur der Pilzkörper des Insektenhirns. III. Die Anatomie der Nervenfasern in den Corpora pedunculata bei *Acheta domesticus* L.: (Orthoptera): Eine Golgi-Studie. Z Zellforsch 145:247–285.

Schürmann F-W. 1974. Bemerkungen zur Funktion der Corpora pedunculata im Gehirn der Insekten aus morphologischer Sicht. Exp Brain Res 19:406–432.

Schürmann F-W. 1987. The architecture of the mushroom bodies and related neuropiles in the insect brain. In: Gupta AP, editor. Arthropod brain: Its evolution, development, structure and functions. New York: John Wiley & Sons. p 231–264.

Schürmann F-W. 2000. Acetylcholine, GABA, glutamate and NO as putative transmitters indicated by immunocytochemistry in the olfactory mushroom body system of the insect brain. Acta Biol Hung 51:355–362.

Schürmann F-W, Erber J. 1990. FMRFamide like immunoreactivity in the brain of the honey bee (*Apis mellifera*). A light and electron microscopical study. Neuroscience 38:797–807.

Schürmann F-W, Ottersen OP, Honegger HW. 2000. Glutamate-like immunoreactivity marks compartments of the mushroom bodies in the brain of the cricket. J Comp Neurol 418:227–239.

Schwärzel M, Müller U. 2006. Dynamic memory networks: dissecting molecular mechanisms underlying associative memory in the temporal domain. Cell Mol Life Sci 63:989–998.

Scotto-Lomassese S, Strambi C, Strambi A, Aouane A, Augier R, Rougon G, Cayre M. 2003. Suppression of adult neurogenesis impairs olfactory learning and memory in an adult insect. J Neurosci 23:9289–9296.

Seid M, Harris KM, Traniello JAF. 2005. Age related changes in the number and structure of synapses in the lip region of the mushroom bodies in the ant *Pheidole dentata*. J Comp Neurol 488:269–277.

Sinakevitch I, Farris SM, Strausfeld NJ. 2001. Taurine-, aspartate-, and glutamate-like immunoreactivity identifies chemically distinct subdivisions of Kenyon cells in the cockroach mushroom body. J Comp Neurol 439:352–367.

Strambi C, Cayre M, Satelle DB, Augier R, Charpin P, Strambi A. 1998. Immunocytochemical mapping of an RDL-like GABA-receptor subunit and of GABA in brain structures related to learning and memory in the cricket *Acheta domesticus*. Learn Mem 5:78–88.

Strausfeld NJ. 1976. Atlas of an insect brain. Berlin: Springer Verlag.

Strausfeld NJ. 2002. Organization of the honey bee mushroom body: representation of the calyx within the vertical and gamma lobes. J Comp Neurol 450:4–33.

Strausfeld NJ, Hansen L, Li Y, Gomez RS, Ito K. 1998. Evolution, discov-

ery, and interpretations of arthropod mushroom bodies. Learn Mem 5:11–37.

Strausfeld NJ, Homberg U, Kloppenburg P. 2000. Parallel organization in honey bee mushroom bodies by peptidergic Kenyon cells. J Comp Neurol 424:179–195.

Strausfeld NJ, Sinakevitch I, Vilinsky I. 2003. The mushroom bodies of *Drosophila melanogaster*: an immunocytological and Golgi study of Kenyon cell organization in the calyces and lobes. Microsc Res Techniq 62:151–169.

Taupin P, Gage FH. 2002. Adult neurogenesis and neural stem cells of the central nervous system. J Neurosci Res 69:745–749.

Technau G. 1984. Fiber number in the mushroom bodies of adult *Drosophila melanogaster* depends on age, sex, and experience. J Neurogenet 1:113–126.

Technau G, Heisenberg M. 1982. Neural reorganization during metamorphosis of the corpora pedunculata in *Drosophila melanogaster*. Nature 295:405–407.

Tolbert LP, Oland LA. 1990. Glial cells form boundaries for developing insect olfactory glomeruli. Exp Neurol 109:19–28.

Tucker ES, Oland LA, Tolbert LP. 2004. In vitro analyses of interactions between olfactory receptor growth cones and glial cells that mediate axon sorting and glomerulus formation. J Comp Neurol 472:478–495.

Voronezhskaya EE, Tsitrin EB, Nezlin LP. 2002. Neuronal development in the larval polychaete *Phyllodoce maculata* (Phyllodocidae). J Comp Neurol 455:299–309.

Watson AHD, Schürmann F-W. 2002. Synaptic structure, distribution, and circuitry in the central nervous system of the locust and related insects. Microsc Res Techniq 56:210–226.

Watts RJ, Hoopfer ED, Luo L. 2003. Axon pruning during *Drosophila* metamorphosis: evidence for local degeneration and requirement of the ubiquitin-proteasome system. Neuron 38:871–885.

Watts RJ, Schuldiner O, Perrino J, Larsen C, Luo L. 2004. Glia engulf degenerating axons during developmental axon pruning. Curr Biol 14:678–684.

Xia S, Miyashita T, Fu TF, Lin WY, Saitoe M, Tully T, Chiang AS. 2005. NMDA receptors mediate olfactory learning and memory in *Drosophila*. Curr Biol 15:603–615.

Yasuyama K, Meinertzhagen IA, Schürmann F-W. 2002. Synaptic organization of the mushroom body calyx in *Drosophila melanogaster*. J Comp Neurol 445:211–226.

Zhu S, Chiang AS, Lee T. 2003. Development of the *Drosophila* mushroom bodies. Elaboration, remodeling and spatial organization of dendrites in the calyx. Development 130:2603–2610.